Emission efficiency of cationic solid state luminophores is directly proportional to intermolecular charge transfer intensity

Kaspars Leduskrasts, Artis Kinens, Edgars Suna*

Latvian Institute of Organic Synthesis, Aizkraukles 21, LV-1006, Riga, Latvia

edgars@osi.lv

Contents

General considerations

Column chromatography was performed using reversed phase C18-silica gel columns (RP18 25-40 μm) and direct phase silica gel columns.

Nuclear magnetic resonance spectra were recorded on NMR spectrometers at the following frequencies: ^{1}H, 400 MHz, 300 MHz; ^{13}C{^{1}H}, 101 MHz. Chemical shifts are reported in parts per million (ppm) relative to TMS or with the residual solvent peak as an internal reference. High-resolution mass spectra (HRMS (ESI-TOF)) were recorded on a mass spectrometer with a time-of-flight (TOF) mass analyzer using the ESI technique. Melting points are uncorrected.

Unless otherwise noted, all chemicals were used as received from commercial sources. Anhydrous THF was obtained by passing commercially available solvent through activated alumina columns.

The luminescence data was collected with Edinburgh Instruments *FS5* Spectrofluorometer; photoluminescence quantum yields (Φ) were measured using an integrating sphere.

Single-crystal X-ray diffraction analyses were performed on Rigaku *XtaLAB Synergy S, Dualflex* apparatus with HyPix6000 detector and CuK_{α} /MoK_{α} radiation type.

Synthesis of emitters 1–4

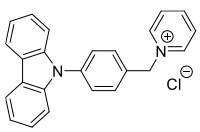

1-(4-(9*H*-Carbazol-9-yl)benzyl)pyridin-1-ium chloride (**1**) was synthesized according to a published protocol.[1] The ^{1}H NMR was fully consistent with the previous report.[1]

^{1}H NMR (300 MHz, $(CD_3)_2SO$, ppm) δ 9.42–9.34 (m, 2H), 8.73–8.65 (m, 1H), 8.30–8.22 (m, 4H), 7.90–7.82 (m, 2H), 7.78–7.71 (m, 2H), 7.48–7.36 (m, 4H), 7.34–7.26 (m, 2H), 6.06 (s, 2H).

Synthesis of emitter 2a

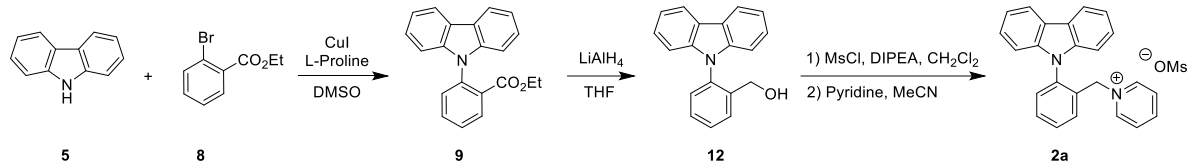

Ethyl 2-(9*H*-carbazol-9-yl)benzoate (**9**). Anhydrous DMSO (21 mL) was added *via* septa to a mixture of 9*H*-carbazole (**5**, 1.0 g, 6.0 mmol, 1.0 equiv), ethyl 2-bromobenzoate (**8**, 1.6 g, 7.2 mmol, 1.2 equiv), CuI (0.2 g, 0.9 mmol, 0.15 equiv), L-Proline (0.2 g, 1.8 mmol, 0.3 equiv) and K_2CO_3 (2.5 g, 18 mmol, 3.0 equiv) in an argon-purged 100 mL round-bottom flask. The flask was sealed with rubber septa and heated at 140 ºC for 72h. After cooling, the black suspension was diluted with water (100 mL), saturated aqueous ammonia (50 mL) and CH_2Cl_2 (50 mL). Phases were separated, and the water phase was extracted with CH_2Cl_2 (2×50 mL). The combined organic layers were dried over anhydrous Na_2SO_4 and purified by silica gel column chromatography using 1:30 (v/v) EtOAc:petroleum ether as the mobile phase to obtain **9** as a colorless solid (1.1 g, 58%); analytical TLC on silica gel, 1:30 EtOAc/petroleum ether, R_f =0.15. Analytically pure material was obtained by crystallization from EtOAc/hexane: mp 106–107 °C (colorless rectangles).

^{1}H NMR (400 MHz, $CDCl_3$, ppm) δ 8.17–8.13 (m, 3H), 7.79–7.73 (m, 1H), 7.65–7.57 (m, 2H), 7.42–7.36 (m, 2H), 7.30–7.25 (m, 2H), 7.16–7.12 (m, 2H), 3.66 (q, *J*=7.1 Hz, 2H), 0.39 (t, *J*=7.1 Hz, 3H).

^{13}C{^{1}H} NMR (101 MHz, $CDCl_3$, ppm) δ 166.3, 141.8, 136.8, 133.4, 132.3, 130.9, 130.4, 128.6, 126.0, 123.3, 120.3, 119.9, 109.5, 61.2, 13.0.

HRMS m/z: $[M]^+$ calculated for $C_{21}H_{18}NO_2^+$: 316.1332; Found: 316.1331.

IR (KBr, cm^{-1}) 1720 (C=O).

(2-(9*H*-Carbazol-9-yl)phenyl)methanol (**12**). Anhydrous THF (10 mL) solution of to ethyl 2-(9*H*-carbazol-9-yl)benzoate (**9**, 1.0 g, 3.2 mmol, 1.0 equiv) was added to an anhydrous THF (10 mL) suspension of $LiAlH_4$ (0.5 g, 13 mmol, 4.0 equiv) in a sealed, Ar flushed 100 mL roundbottom flask at 0 °C. The sealed flask was heated at 70 °C for 1h. The reaction mixture was cooled and quenched by drop wise addition of water until gas evolution ceased, followed by addition of water (2 mL) and 15% aqueous NaOH solution (0.6 mL). The obtained suspension was filtered through a pad of ceilte, washed with EtOAc. The filtrate was dried over anhydrous Na_2SO_4 and the organics evaporated to yield the product **12** as a colorless amorphous material (0.85 g, 98 %).

^{1}H NMR (400 MHz, $CDCl_3$, ppm) δ 8.19–8.14 (m, 2H), 7.82–7.78 (m, 1H), 7.63–7.57 (m, 1H), 7.55–7.50 (m, 1H), 7.42–7.36 (m, 3H), 7.32–7.27 (m, 2H), 7.06–7.02 (m, 2H), 4.34 (d, *J*=4.4 Hz, 2H), 1.53–1.47 (m, 1H).

^{13}C{^{1}H} NMR (101 MHz, $CDCl_3$, ppm) δ 141.6, 140.1, 134.8, 129.6, 129.4, 129.3, 129.2, 126.3, 123.2, 120.6, 120.0, 109.7, 61.1.

HRMS m/z: $[M]^+$ calculated for $C_{19}H_{15}NO^+$: 273.1154; Found: 273.1153.

IR (KBr, cm^{-1}) 3447 (O–H).

1-(2-(9*H*-Carbazol-9-yl)benzyl)pyridin-1-ium methanesulfonate (**2a**). Anhydrous CH_2Cl_2 (30 mL) was added to (2-(9*H*-carbazol-9-yl)phenyl)methanol (**12**, 0.85 g, 3.1 mmol, 1.0 equiv) in a 50 mL roundbottom flask at 0 °C. To the cooled colorless solution MsCl (0.5 mL, 6.2 mmol, 2.0 equiv) followed by DIPEA (2.2 mL, 12 mmol, 4.0 equiv) was added. The pale yellow solution was stirred in an ice bath. After 1h the reaction mixture was diluted with CH_2Cl_2 (50 mL) and H_2O (50 mL), the layers seperated and the water layer washed with CH_2Cl_2 (30 mL) one more time. The combined organics were dried over Na_2SO_4 and evaporated to give a yellow oil. MeCN (15 mL) was added to the yellow oil to form a yellow solution. Pyridine (0.8 mL, 9.3 mmol, 3.0 equiv) was added to the yellow solution and stirred at room temperature. After 72h the reaction mixture was diluted with EtOAc (150 mL) and stirred at 0 °C. After 1h the resulting precipitate was filtered and washed with EtOAc and Et_2O to give the product **2a** as a pale green solid (1.0 g, 75%). Analytically pure material was obtained by crystallization from MeCN/EtOAc: mp 227–228 °C (colorless plates).

^{1}H NMR (400 MHz, $(CD_3)_2SO$, ppm) δ 8.25–8.14 (m, 5H), 7.89–7.83 (m, 1H), 7.82–7.76 (m, 2H), 7.64–7.58 (m, 2H), 7.57–7.51 (m, 1H), 7.36–7.25 (m, 4H), 6.88–6.82 (m, 2H), 5.60 (s, 2H), 2.30 (s, 3H).

$^{13}C\{^1H\}$ NMR (101 MHz, $(CD_3)_2SO$, ppm) δ 145.2, 143.8, 140.0, 135.4, 133.1, 132.4, 132.1, 130.7, 130.2, 127.5, 126.5, 122.5, 120.8, 120.4, 109.1, 60.8, 39.8.

HRMS m/z: $[M]^+$ calculated for $C_{24}H_{19}N_2^+$: 335.1543; Found: 335.1556.

IR (KBr, cm^{-1}) 1193 (S=O).

Synthesis of compound 2b

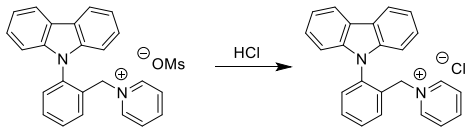

1-(2-(9*H*-Carbazol-9-yl)benzyl)pyridin-1-ium chloride (**2b**). EtOH (6 mL) was added to 1-(2-(9*H*-carbazol-9-yl)benzyl)pyridin-1-ium methanesulfonate (**2a**, 0.20 g, 0.47 mmol). The pale green solution was subjected to reversed phase column chromatography using 0.1% HCl acidic water and MeCN as an eluent at a rate of 40 mL/min. Initial elution for 20 minutes with 5% MeCN followed by a 40 minute gradient from 5% to 95% MeCN afforded the desired material. After evaporation in *vacuo* the obtained oil was dissolved in MeCN (5 mL) to which EtOAc (50 mL) was slowly added. The formed precipitate was filtered, washed with EtOAc to give the product **2b** as a colorles crystals (0.16 g, 90%). Analytically pure material was obtained by crystallization from MeCN/Et_2O: mp 212–214 °C (colorless prisms).

^1H NMR (400 MHz, $(CD_3)_2SO$, ppm) δ 8.21–8.16 (m, 2H), 8.12–8.07 (m, 1H), 8.06–8.01 (m, 2H), 7.91–7.86 (m, 1H), 7.82–7.75 (m, 2H), 7.54–7.48 (m, 3H), 7.34–7.24 (m, 4H), 6.83–6.77 (m, 2H), 5.56 (s, 2H).

$^{13}C\{^1H\}$ NMR (101 MHz, $(CD_3)_2SO$, ppm) δ 145.3, 143.7, 140.2, 135.7, 133.3, 133.0, 132.6, 131.0, 130.6, 127.7, 127.0, 122.7, 121.1, 120.9, 109.3, 61.3.

HRMS m/z: $[M]^+$ calculated for $C_{24}H_{19}N_2^+$: 335.1543; Found: 335.1551.

IR (KBr, cm^{-1}) 3049 (C–H).

Synthesis of emitter 3

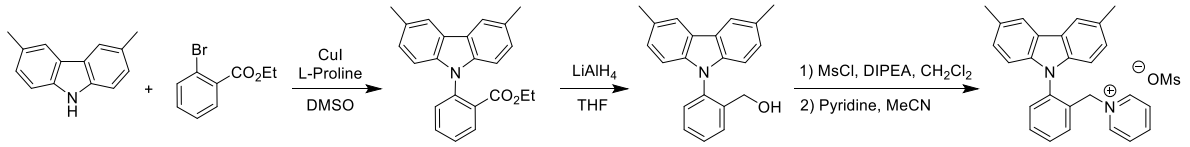

6 8 10 13 3

Ethyl 2-(3,6-dimethyl-9*H*-carbazol-9-yl)benzoate (**10**). Anhydrous DMSO (21 mL) was added *via* septa to a mixture of 3,6-dimethyl-9*H*-carbazole (**6**, 0.8 g, 4.3 mmol, 1.0 equiv), ethyl 2-bromobenzoate (**8**, 1.3 g, 5.5 mmol, 1.3 equiv), CuI (0.1 g, 0.6 mmol, 0.15 equiv), L-Proline (0.1 g, 1.3 mmol, 0.3 equiv) and K_2CO_3 (1.8 g, 13 mmol, 3.0 equiv) in an argon-purged 100 mL round-bottom flask. The flask was sealed with rubber septa and heated at 140 ^oC for 72h. After cooling, the black suspension was diluted with water (100 mL), saturated aqueous ammonia (50 mL) and CH_2Cl_2 (50 mL). Phases were separated, and the water phase was extracted with CH_2Cl_2 (2×50 mL). The combined organic layers were dried over anhydrous Na_2SO_4 and purified by silica gel column chromatography using 1:30 (v/v) EtOAc:petroleum ether as the mobile phase to obtain **10** as a viscous oil (1.0 g, 71%); analytical TLC on silica gel, 1:10 EtOAc/petroleum ether, R_f=0.40.

^{1}H NMR (400 MHz, $CDCl_3$, ppm) δ 8.12–8.08 (m, 1H), 7.90–8.87 (m, 2H), 7.75–7.69 (m, 1H), 7.60–7.53 (m, 2H), 7.19–7.15 (m, 2H), 7.03–6.99 (m, 2H), 3.68 (q, *J*=7.1 Hz, 2H), 2.53 (s, 6H) 0.45 (t, *J*=7.1 Hz, 3H).

^{13}C{^{1}H} NMR (101 MHz, $CDCl_3$, ppm) δ 166.5, 140.3, 137.3, 133.3, 132.1, 130.8, 130.2, 128.9, 128.2, 127.2, 123.4, 120.2, 109.1, 61.2, 21.6, 13.0.

HRMS m/z: $[M]^+$ calculated for $C_{23}H_{22}NO_2^+$: 344.1651; Found: 344.1656.

IR (KBr, cm^{-1}) 1713 (C=O).

(2-(3,6-Dimethyl-9*H*-carbazol-9-yl)phenyl)methanol (**13**). Anhydrous THF (10 mL) solution of to ethyl 2-(3,6-dimethyl-9*H*-carbazol-9-yl)benzoate (**10**, 0.8 g, 2.3 mmol, 1.0 equiv) was added to an anhydrous THF (10 mL) suspension of $LiAlH_4$ (0.4 g, 9.3 mmol, 4.0 equiv) in a sealed, Ar flushed 100 mL roundbottom flask at 0 ^oC. The sealed flask was heated at 70 ^oC for 1h. The reaction mixture was cooled and quenched by drop wise addition of water until gas evolution ceased, followed by addition of water (1.5 mL) and 15% aqueous NaOH solution (0.4 mL). The obtained suspension was filtered through a pad of ceilte, washed with EtOAc. The filtrate was dried over anhydrous Na_2SO_4 and the organics evaporated to yield the product **13** as a viscous oil (0.67 g, 95 %).

^{1}H NMR (400 MHz, $CDCl_3$, ppm) δ 7.95–7.91 (m, 2H), 7.80–7.75 (m, 1H), 7.60–7.54 (m, 1H), 7.53–7.47 (m, 1H), 7.38–7.33 (m, 1H), 7.22–7.16 (m, 2H), 6.94–6.89 (m, 2H), 4.33 (s, 2H), 2.55 (s, 6H).

^{13}C{^{1}H} NMR (101 MHz, $CDCl_3$, ppm) δ 140.2, 140.1, 135.3, 129.5, 129.3, 129.2, 129.1, 127.4, 123.2, 120.5, 109.3, 61.2, 21.5.

HRMS m/z: $[M]^+$ calculated for $C_{21}H_{19}NO^+$: 301.1467; Found: 301.1469.

IR (KBr, cm^{-1}) 3376 (O–H).

1-(2-(3,6-Dimethyl-9*H*-carbazol-9-yl)benzyl)pyridin-1-ium methanesulfonate (**3**). Anhydrous CH_2Cl_2 (30 mL) was added to (2-(3,6-dimethyl-9*H*-carbazol-9-yl)phenyl)methanol (**13**, 0.6 g, 2.0 mmol, 1.0 equiv) in a 50 mL roundbottom flask at 0 ºC. To the cooled colorless solution MsCl (0.3 mL, 4.0 mmol, 2.0 equiv) followed by DIPEA (1.4 mL, 8.0 mmol, 4.0 equiv) was added. The pale yellow solution was stirred in an ice bath. After 1h the reaction mixture was diluted with CH_2Cl_2 (50 mL) and H_2O (50 mL), the layers seperated and the water layer washed with CH_2Cl_2 (30 mL) one more time. The combined organics were dried over Na_2SO_4 and evaporated to give a yellow oil. MeCN (15 mL) was added to the yellow oil to form a yellow solution. Pyridine (1.6 mL, 20 mmol, 10 equiv) was added to the yellow solution and stirred at room temperature. After 72h the reaction mixture was diluted with Et_2O (150 mL) and stirred at 0 ºC. After 1h the resulting precipitate was filtered and washed with Et_2O to give the product **3** as a colorless solid (0.84 g, 92%). Analytically pure material was obtained by crystallization from MeCN/Et_2O: decomposition 230–250 °C (colorless prisms).

^{1}H NMR (400 MHz, CD_3OD, ppm) δ 8.00–7.94 (m, 2H), 7.90–7.88 (m, 2H), 7.84–7.76 (m, 4H), 7.55–7.50 (m, 1H), 7.39–7.33 (m, 2H), 7.14–7.11 (m, 2H), 6.70–6.65 (m, 2H), 5.56 (s, 2H), 2.67 (s, 3H), 2.51 (s, 6H).

^{13}C{^{1}H} NMR (101 MHz, CD_3OD, ppm) δ 145.7, 144.2, 139.7, 137.6, 134.4, 134.3, 133.6, 132.4, 131.4, 131.2, 128.8, 128.5, 124.2, 121.6, 109.7, 63.5, 39.5, 21.4.

HRMS m/z: $[M]^+$ calculated for $C_{26}H_{23}N_2^+$: 363.1861; Found: 363.1861.

IR (KBr, cm^{-1}) 1192 (S=O).

Synthesis of emitter 4a

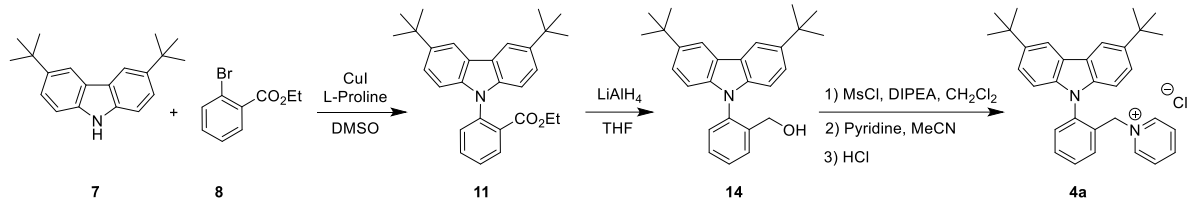

Ethyl 2-(3,6-di-*tert*-butyl-9*H*-carbazol-9-yl)benzoate (**11**). Anhydrous DMSO (18 mL) was added *via* septa to a mixture of 3,6-di-tert-butyl-9*H*-carbazole (**7**, 1.4 g, 5.0 mmol, 1.0 equiv), ethyl 2-bromobenzoate (**8**, 1.5 g, 6.5 mmol, 1.3 equiv), CuI (0.1 g, 0.8 mmol, 0.15 equiv), L-Proline (0.2 g, 1.5 mmol, 0.3 equiv) and K_2CO_3 (2.1 g, 15 mmol, 3.0 equiv) in an argon-purged 100 mL round-bottom flask. The flask was sealed with rubber septa and heated at 140 ºC for 72h. After cooling, the black suspension was diluted with water (100 mL), saturated aqueous ammonia (50 mL) and CH_2Cl_2 (50 mL). Phases were separated, and the water phase was extracted with CH_2Cl_2 (2×50 mL). The combined organic layers were dried over anhydrous Na_2SO_4 and purified by silica gel column chromatography using 1:30 (v/v) EtOAc:petroleum ether as the mobile phase to obtain **11** as an amorphous material (1.4 g, 67%); analytical TLC on silica gel, 1:10 EtOAc/petroleum ether, R_f=0.45.

^{1}H NMR (400 MHz, $CDCl_3$, ppm) δ 8.13–8.08 (m, 3H), 7.75–7.69 (m, 1H), 7.59–7.54 (m, 2H), 7.43–7.39 (m, 2H), 7.07–7.02 (m, 2H), 3.69 (q, *J*=7.1 Hz, 2H), 1.45 (s, 18H) 0.42 (t, *J*=7.1 Hz, 3H).

^{13}C{^{1}H} NMR (101 MHz, $CDCl_3$, ppm) δ 166.5, 142.7, 140.3, 137.3, 133.2, 132.1, 130.7, 130.2, 128.1, 123.7, 123.4, 116.3, 108.9, 61.2, 34.9, 32.2, 13.0.

HRMS m/z: $[M]^+$ calculated for $C_{29}H_{34}NO_2^+$: 428.2590; Found: 428.2582.

IR (KBr, cm^{-1}) 1716 (C=O).

(2-(3,6-Di-*tert*-butyl-9*H*-carbazol-9-yl)phenyl)methanol (**14**). Anhydrous THF (10 mL) solution of to ethyl ethyl 2-(3,6-di-tert-butyl-9*H*-carbazol-9-yl)benzoate (**11**, 1.2 g, 2.8 mmol, 1.0 equiv) was added to an anhydrous THF (10 mL) suspension of $LiAlH_4$ (0.4 g, 11 mmol, 4.0 equiv) in a sealed, Ar flushed 100 mL roundbottom flask at 0 ºC. The sealed flask was heated at 70 ºC for 1h. The reaction mixture was cooled and quenched by drop wise addition of water until gas evolution ceased, followed by addition of water (2 mL) and 15% aqueous NaOH solution (0.6 mL). The obtained suspension was filtered through a pad of ceilte, washed

with EtOAc. The filtrate was dried over anhydrous Na_2SO_4 and the organics evaporated to yield the product **15** as an amorphous material (0.83 g, 77 %).

^{1}H NMR (400 MHz, $CDCl_3$, ppm) δ 8.18–8.13 (m, 2H), 7.83–7.76 (m, 1H), 7.61–7.54 (m, 1H), 7.53–7.46 (m, 1H), 7.45–7.40 (m, 2H), 7.37–7.32 (m, 1H), 6.98–6.92 (m, 2H), 4.38 (d, *J*=4.9 Hz, 2H), 1.47 (s, 18H).

^{13}C{^{1}H} NMR (101 MHz, $CDCl_3$, ppm) δ 142.9, 140.2, 140.1, 135.4, 129.5, 129.3, 129.2, 129.1, 123.9, 123.2, 116.5, 109.1, 61.3, 34.9, 32.2.

HRMS m/z: $[M]^+$ calculated for $C_{27}H_{31}NO^+$: 385.2406; Found: 385.2411.

IR (KBr, cm^{-1}) 3348 (O–H).

1-(2-(3,6-Di-*tert*-butyl-9*H*-carbazol-9-yl)benzyl)pyridin-1-ium chloride (**4a**). Anhydrous CH_2Cl_2 (30 mL) was added to (2-(3,6-di-tert-butyl-9*H*-carbazol-9-yl)phenyl)methanol (**14**, 0.4 g, 1.0 mmol, 1.0 equiv) in a 50 mL roundbottom flask at 0 ^{o}C. To the cooled colorless solution MsCl (0.2 mL, 2.0 mmol, 2.0 equiv) followed by DIPEA (0.7 mL, 4.0 mmol, 4.0 equiv) was added. The pale yellow solution was stirred in an ice bath. After 1h the reaction mixture was diluted with CH_2Cl_2 (50 mL) and H_2O (50 mL), the layers seperated and the water layer washed with CH_2Cl_2 (30 mL) one more time. The combined organics were dried over Na_2SO_4 and evaporated to give a yellow oil. MeCN (15 mL) was added to the yellow oil to form a yellow solution. Pyridine (0.8 mL, 9.9 mmol, 10 equiv) was added to the yellow solution and stirred at room temperature. After 72h the reaction mixture was directly subjected to reversed phase column chromatography using 0.1% HCl acidic water and MeCN as an eluent at a rate of 40 mL/min. Initial elution for 20 minutes with 5% MeCN followed by a 40 minute gradient from 5% to 95% MeCN afforded the desired material. After evaporation in *vacuo* the obtained oil was dissolved in MeCN (5 mL) to which Et_2O (50 mL) was slowly added. The formed precipitate was filtered, washed with EtOAc to give the product **4a** as a colorles crystals (0.41 g, 86%). Analytically pure material was obtained by crystallization from MeCN/EtOAc: mp 219–220 °C (colorless prisms).

^{1}H NMR (400 MHz, CD_3OD, ppm) δ 8.18–8.16 (m, 2H), 8.02–7.93 (m, 2H), 7.86–7.76 (m, 4H), 7.56–7.51 (m, 1H), 7.41–7.32 (m, 4H), 6.72–6.68 (m, 2H), 5.56 (s, 2H), 1.46 (s, 18H).

^{13}C{^{1}H} NMR (101 MHz, CD_3OD, ppm) δ 145.7, 145.2, 144.3, 139.8, 137.7, 134.4, 133.7, 132.5, 131.3, 128.5, 125.5, 124.1, 117.8, 109.4, 63.4, 35.7, 32.4.

HRMS m/z: $[M]^+$ calculated for $C_{32}H_{35}N_2^+$: 447.2800; Found: 447.2815.

IR (KBr, cm^{-1}) 2957 (C–H).

Synthesis of emitter 4b

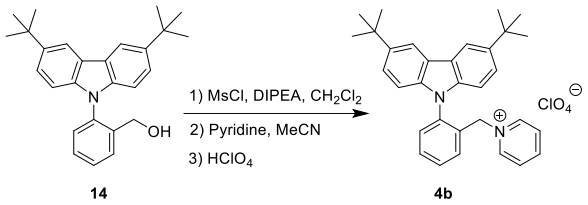

1-(2-(3,6-Di-*tert*-butyl-9*H*-carbazol-9-yl)benzyl)pyridin-1-ium perchlorate (**4b**). Anhydrous CH_2Cl_2 (30 mL) was added to (2-(3,6-di-tert-butyl-9*H*-carbazol-9-yl)phenyl)methanol (**14**, 0.4 g, 1.0 mmol, 1.0 equiv) in a 50 mL roundbottom flask at 0 °C. To the cooled colorless solution MsCl (0.2 mL, 2.0 mmol, 2.0 equiv) followed by DIPEA (0.7 mL, 4.0 mmol, 4.0 equiv) was added. The pale yellow solution was stirred in an ice bath. After 1h the reaction mixture was diluted with CH_2Cl_2 (50 mL) and H_2O (50 mL), the layers seperated and the water layer washed with CH_2Cl_2 (30 mL) one more time. The combined organics were dried over Na_2SO_4 and evaporated to give a yellow oil. MeCN (15 mL) was added to the yellow oil to form a yellow solution. Pyridine (0.8 mL, 9.9 mmol, 10 equiv) was added to the yellow solution and stirred at room temperature. After 72h the reaction mixture was directly subjected to reversed phase column chromatography using 0.1% $HClO_4$ acidic water and MeCN as an eluent at a rate of 40 mL/min. Initial elution for 20 minutes with 5% MeCN followed by a 40 minute gradient from 5% to 95% MeCN afforded the desired material. After evaporation in *vacuo* the obtained oil was crystallized from H_2O (25 mL). The formed precipitate was filtered, washed with H_2O to give the product **4b** as a colorles solid (0.40 g, 73%). Analytically pure material was obtained by crystallization H_2O: mp 198–199 °C (colorless plates).

^{1}H NMR (400 MHz, CD_3OD, ppm) δ 8.00–7.91 (m, 2H), 7.85–7.77 (m, 2H), 7.77–7.73 (m, 2H), 7.55–7.51 (m, 1H), 7.41–7.36 (m, 2H), 7.35–7.30 (m, 2H), 6.72–6.68 (m, 2H), 5.54 (s, 2H), 1.46 (s, 18H).

^{13}C{^{1}H} NMR (101 MHz, CD_3OD, ppm) δ 145.7, 145.2, 144.2, 139.7, 137.7, 134.4, 134.3, 133.7, 132.5, 131.3, 128.5, 125.5, 124.1, 117.8, 109.4, 63.5, 35.7, 32.4.

HRMS m/z: $[M]^+$ calculated for $C_{32}H_{35}N_2^+$: 447.2800; Found: 447.2802.

IR (KBr, cm^{-1}) 2959 (C–H).

Luminescence spectra

Absorption in solution

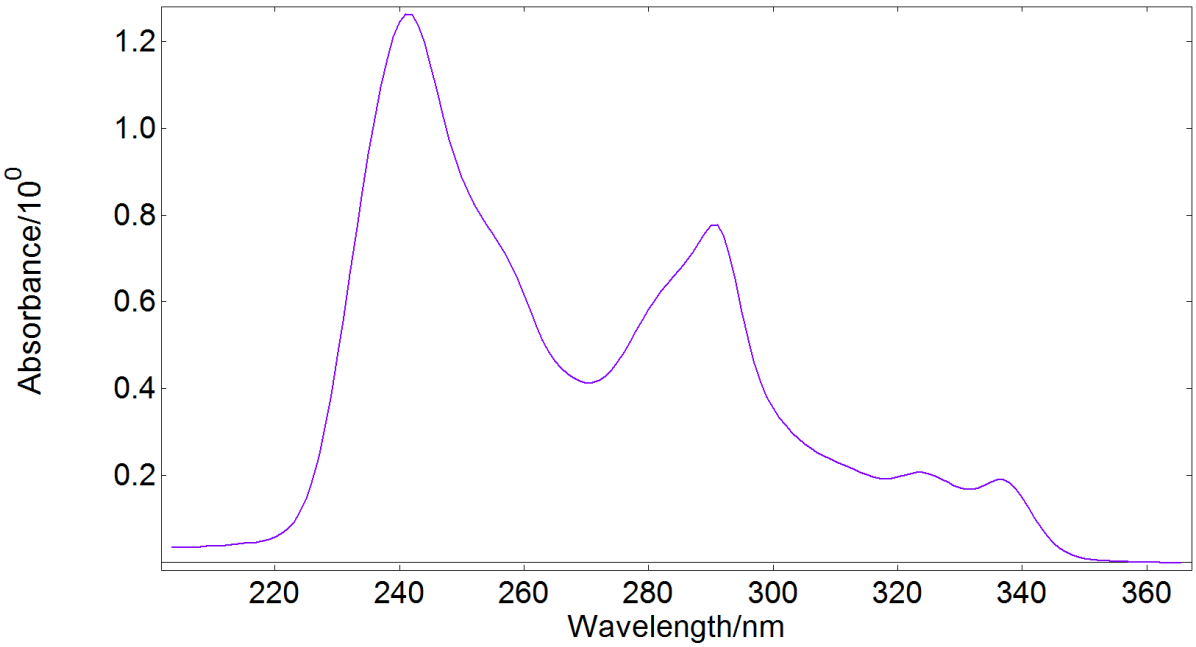

Fig. S1. Absorption of **1** in MeCN solution (at 10^{-5} mol/L)

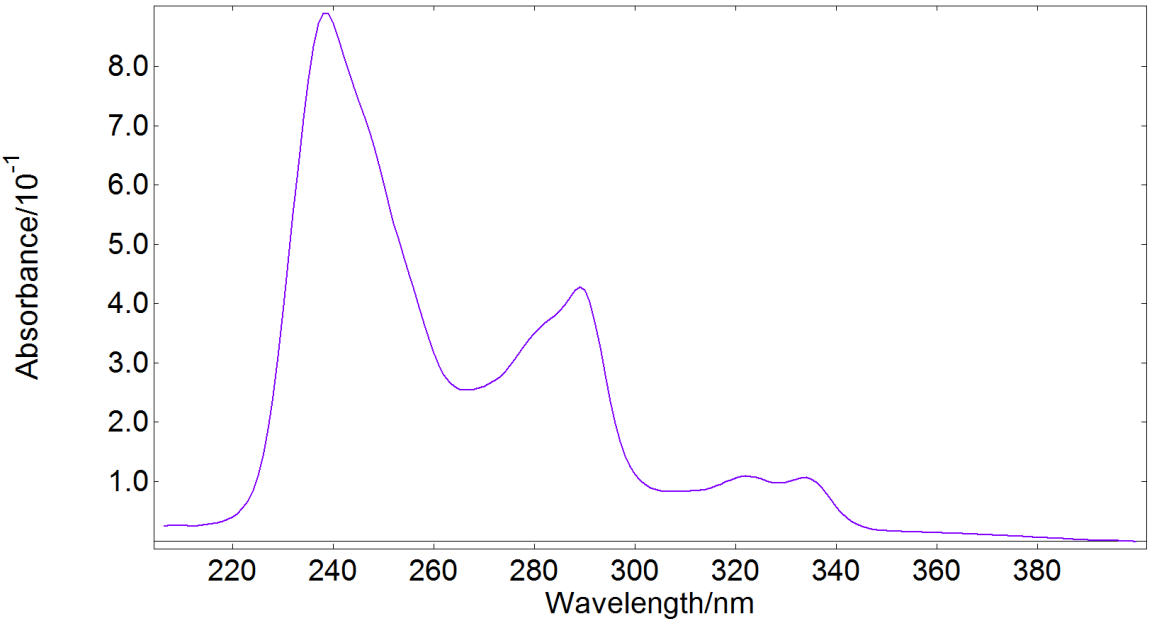

Fig. S2. Absorption of **2a** in MeCN solution (at 10^{-5} mol/L)

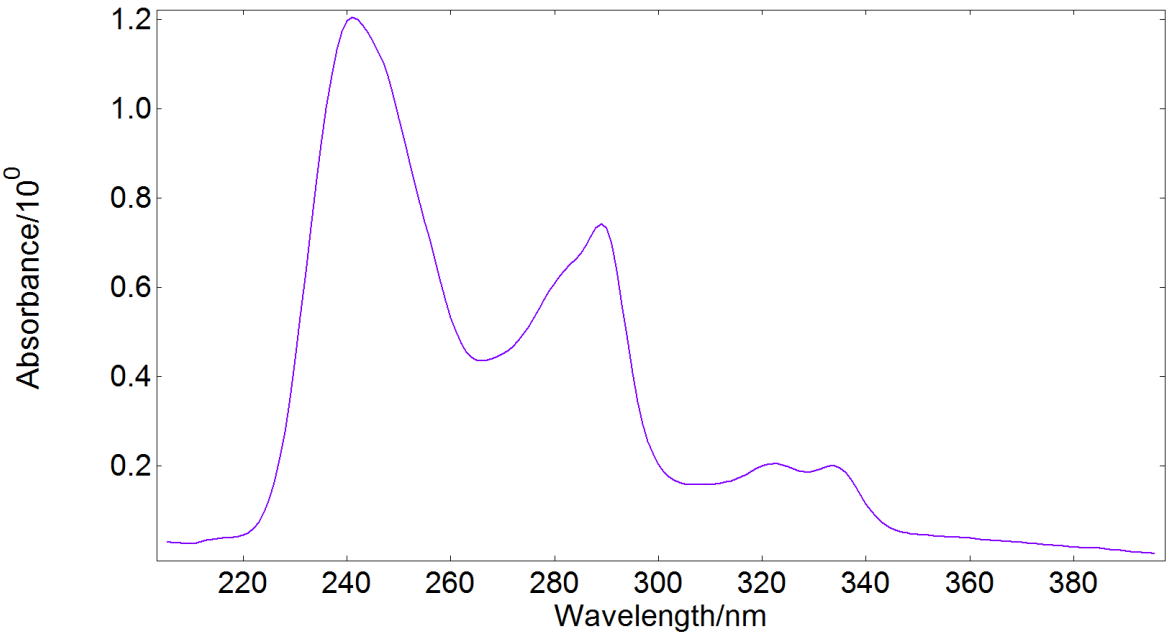

Fig. S3. Absorption of **2b** in MeCN solution (at 10^{-5} mol/L)

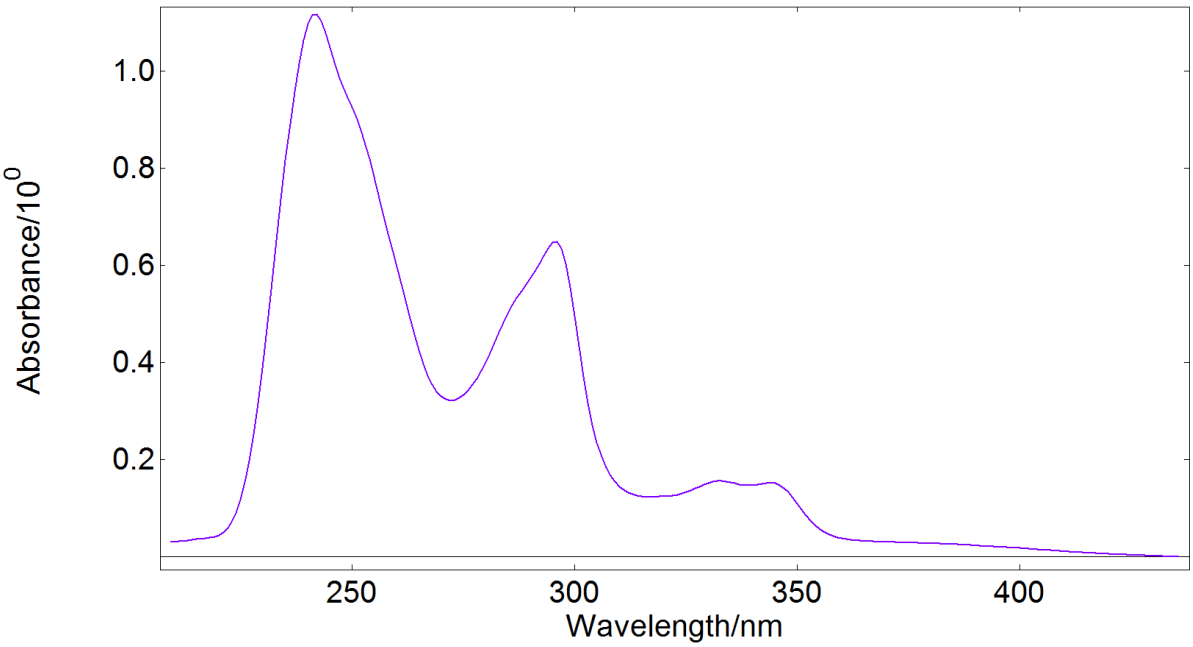

Fig. S4. Absorption of **3** in MeCN solution (at 10^{-5} mol/L)

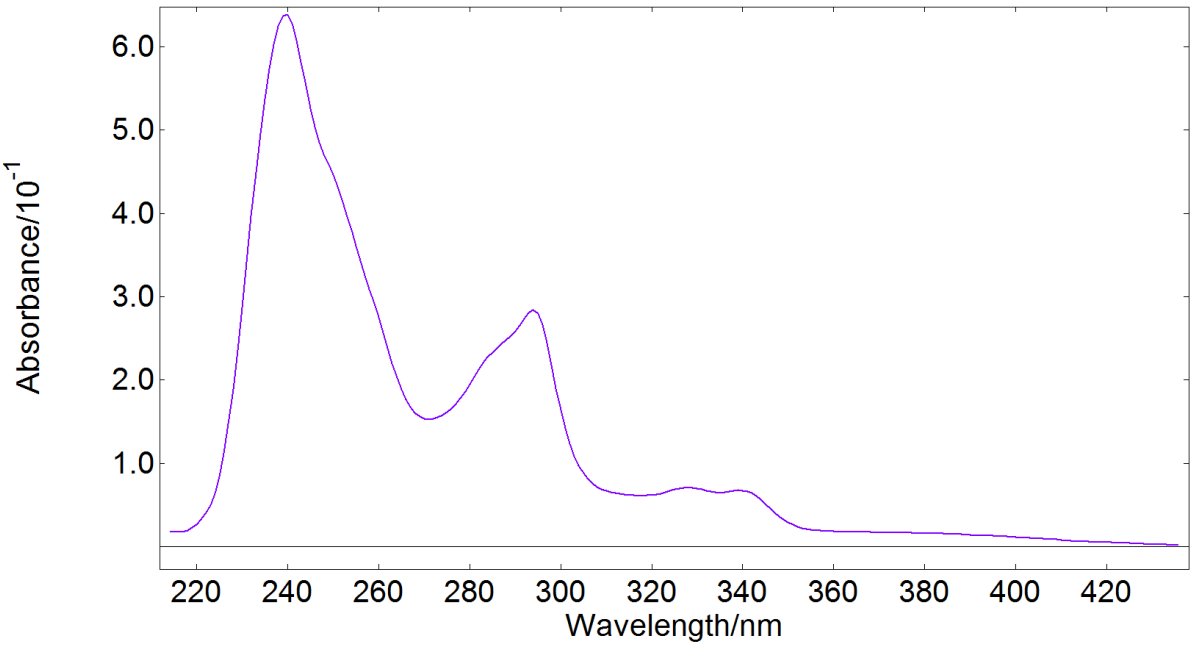

Fig. S5. Absorption of **4a** in MeCN solution (at 10^{-5} mol/L)

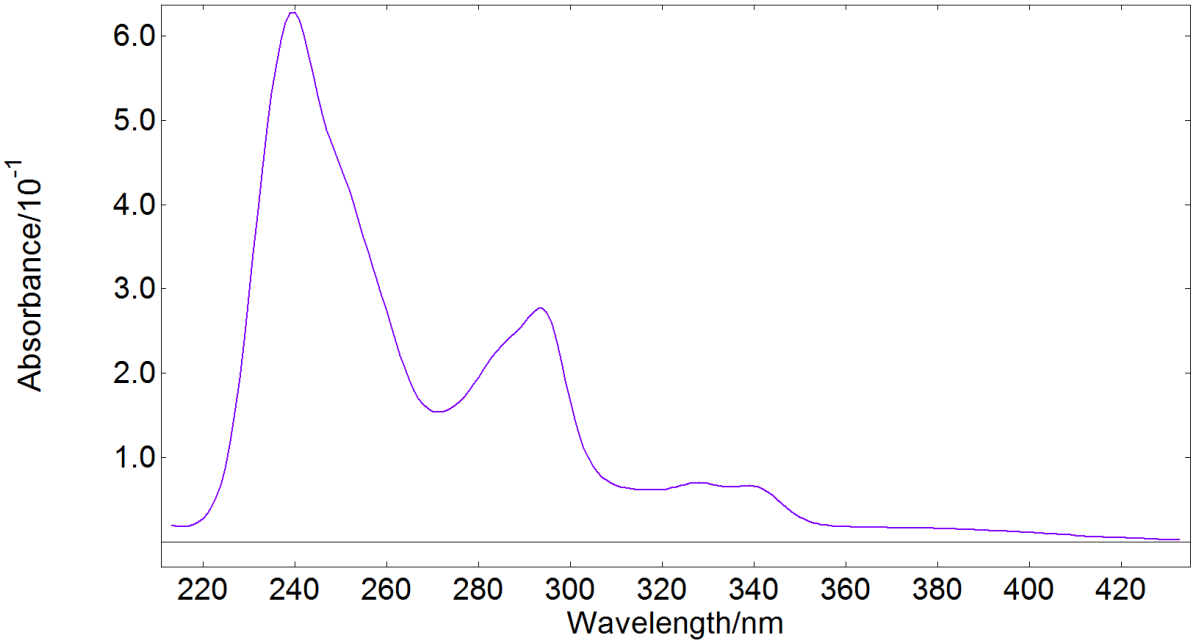

Fig. S6. Absorption of **4b** in MeCN solution (at 10^{-5} mol/L)

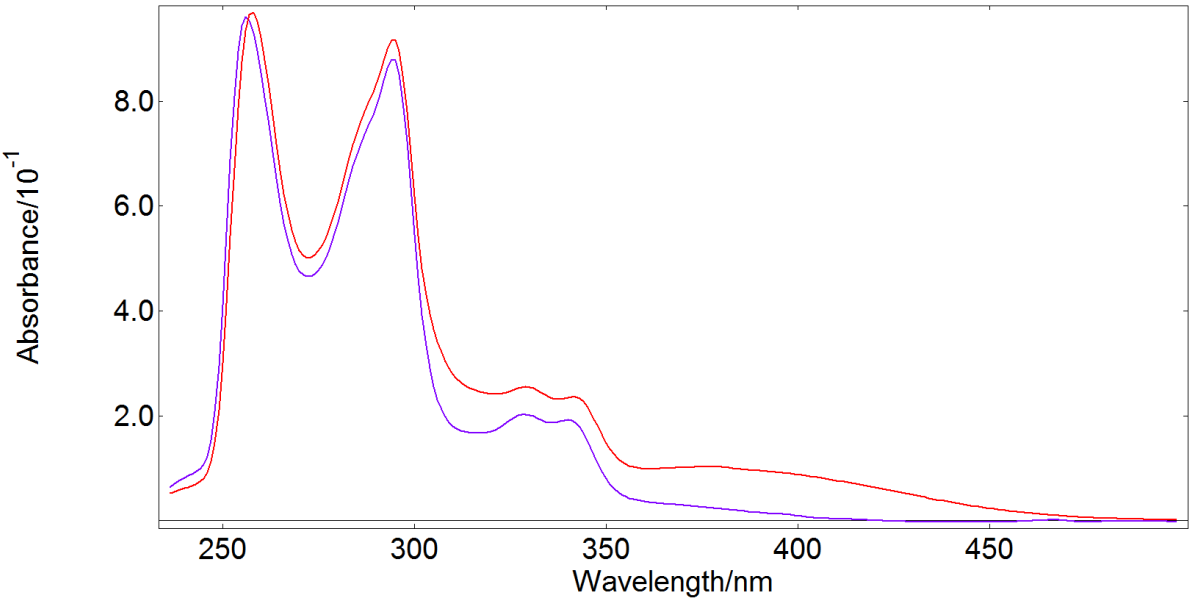

Fig. S7. Absorption of **4b** in EtOAc solution before (blue) and after (red) addition of 2 equivalents tetra-*n*-butylammonium iodide (at 10^{-5} mol/L)

Emission in MeCN solution

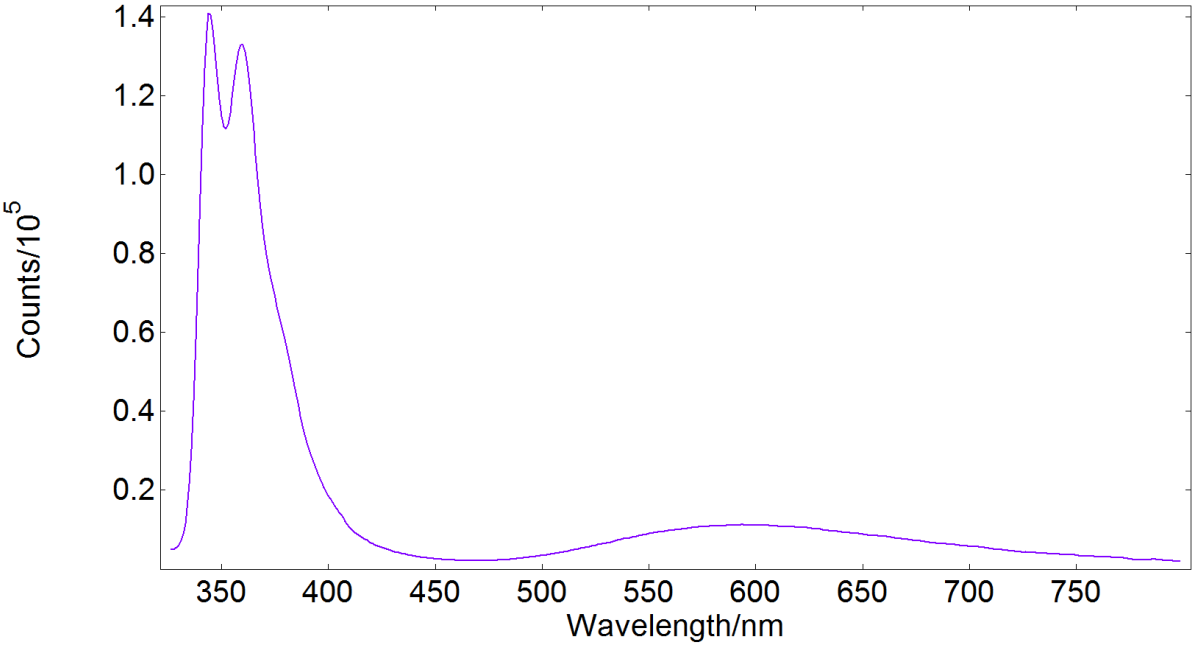

Fig. S8. Emission of **2a** in MeCN solution (at 10^{-5} mol/L)

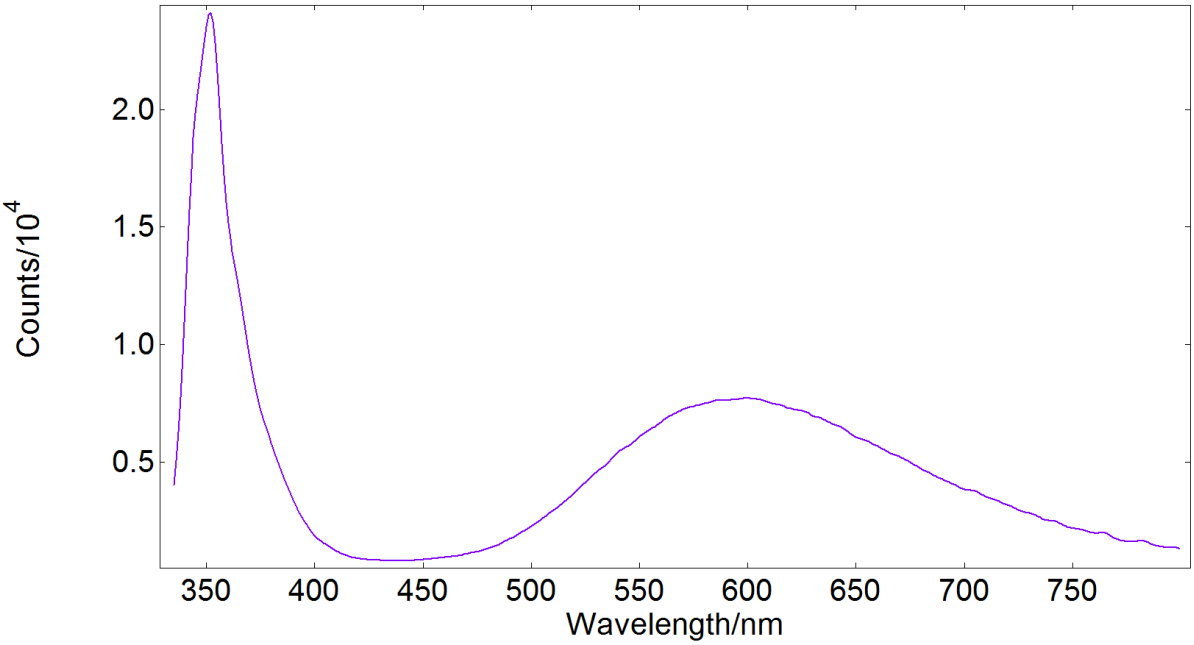

Fig. S9. Emission of **2b** in MeCN solution (at 10^{-5} mol/L)

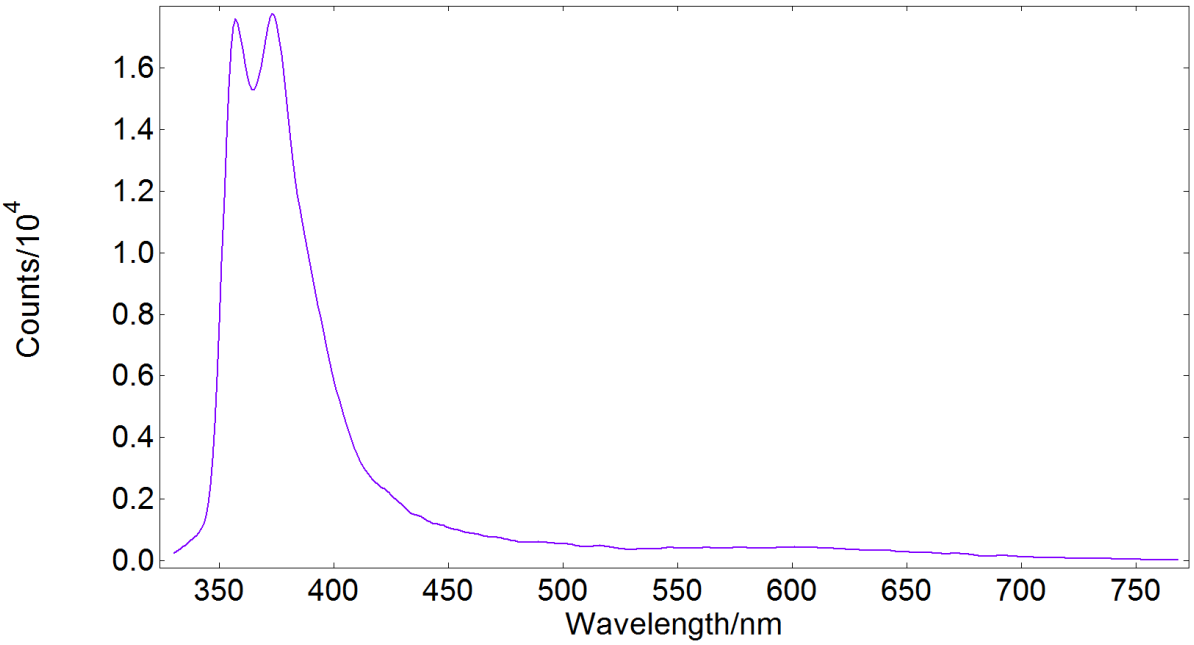

Fig. S10. Emission of **3** in MeCN solution (at 10^{-5} mol/L)

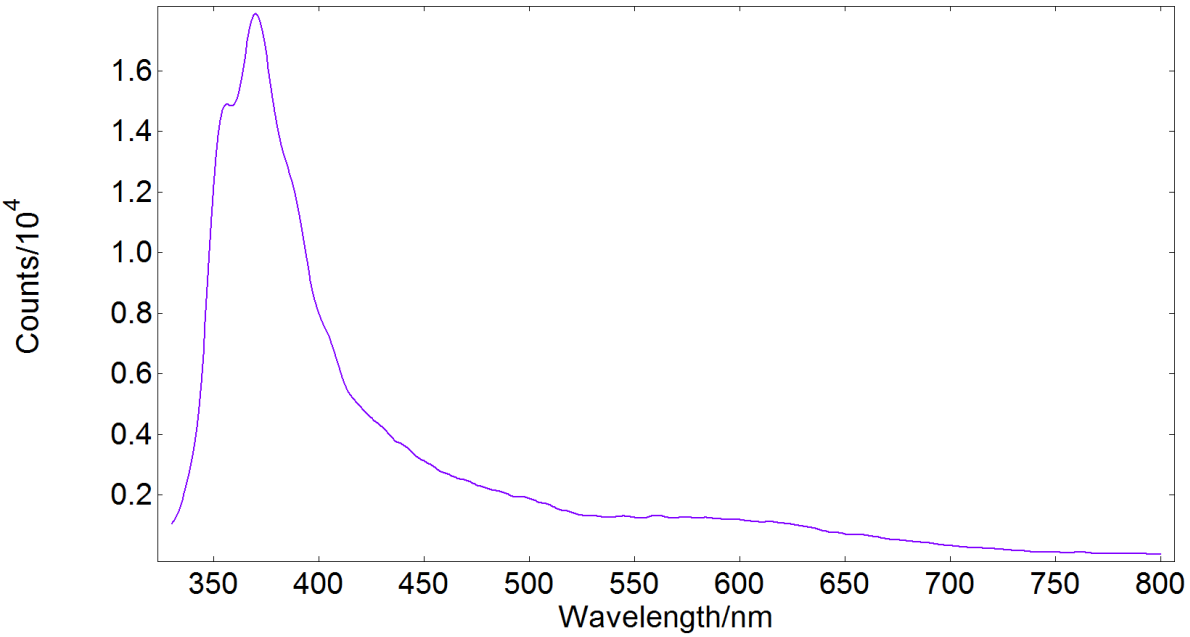

Fig. S11. Emission of **4a** in MeCN solution (at 10^{-5} mol/L)

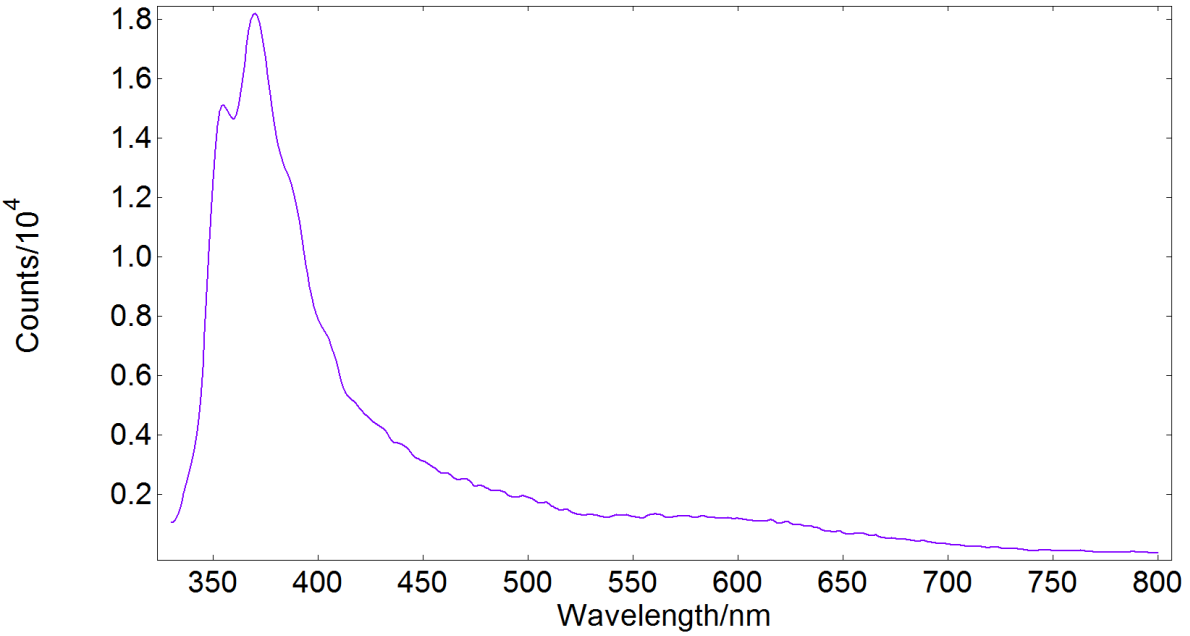

Fig. S12. Emission of **4b** in MeCN solution (at 10^{-5} mol/L)

Emission in the solid state

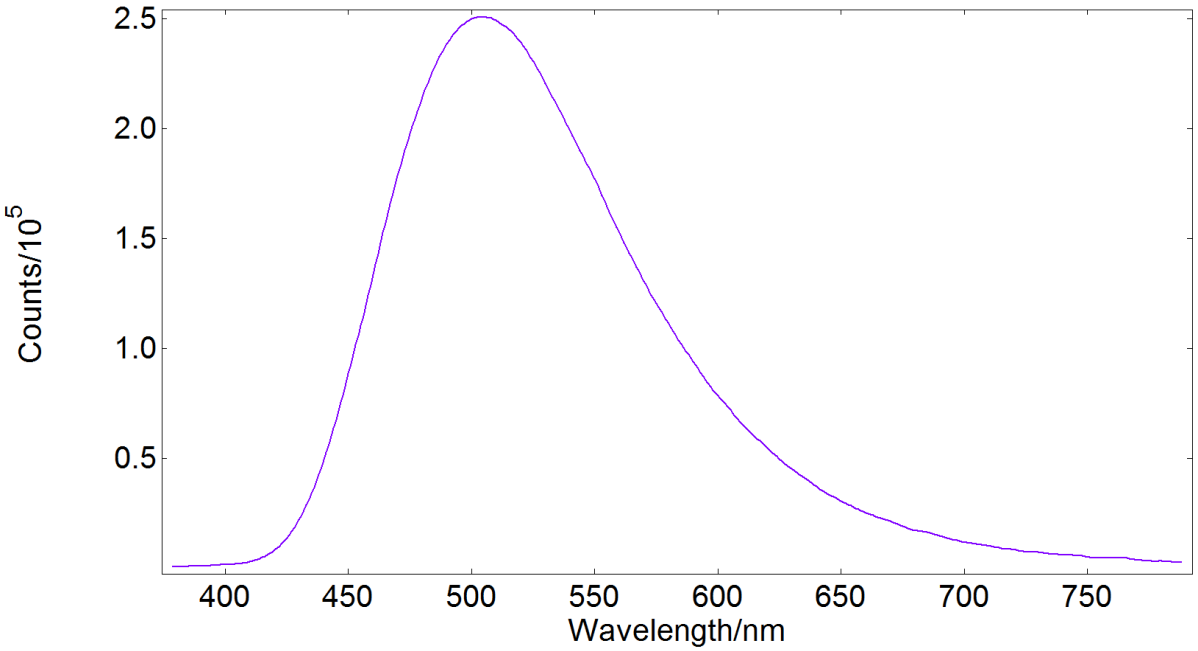

Fig. S13. Emission of **1** in the solid state

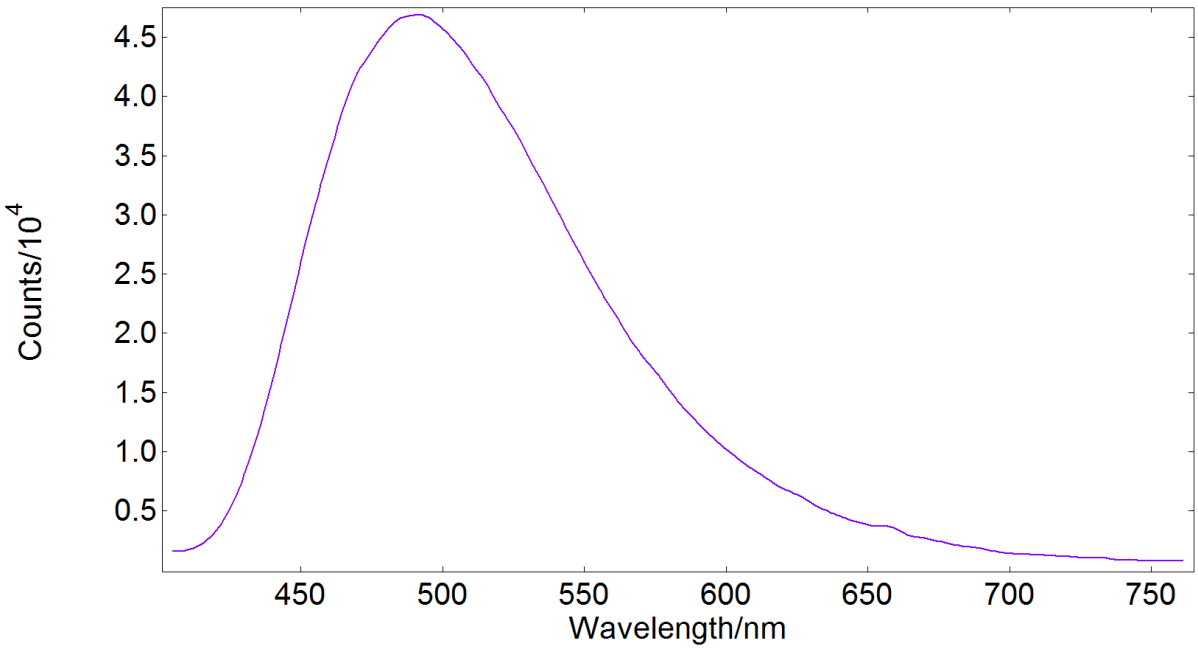

Fig. S14. Emission of **2a** in the solid state

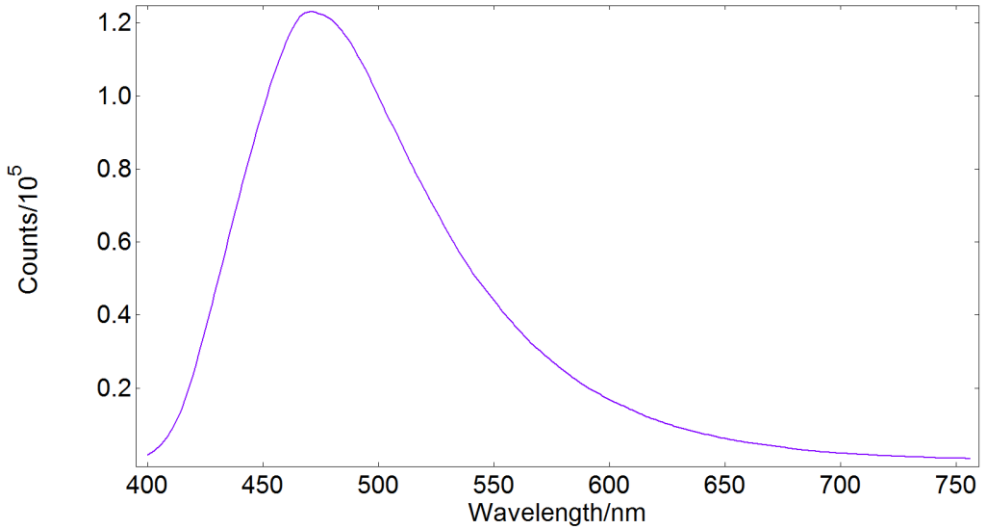

Fig. S15. Emission of **2b** in the solid state

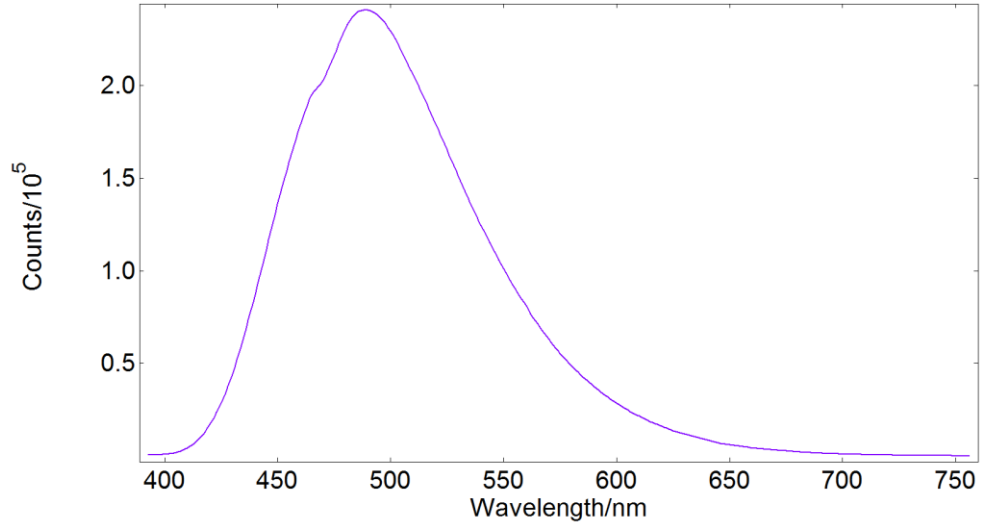

Fig. S16. Emission of **3** in the solid state

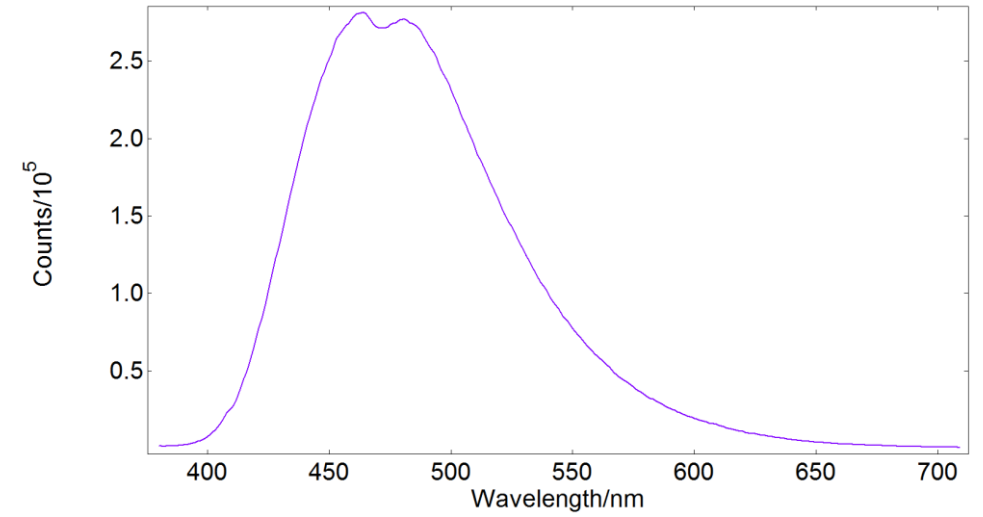

Fig. S17. Emission of **4a** in the solid state

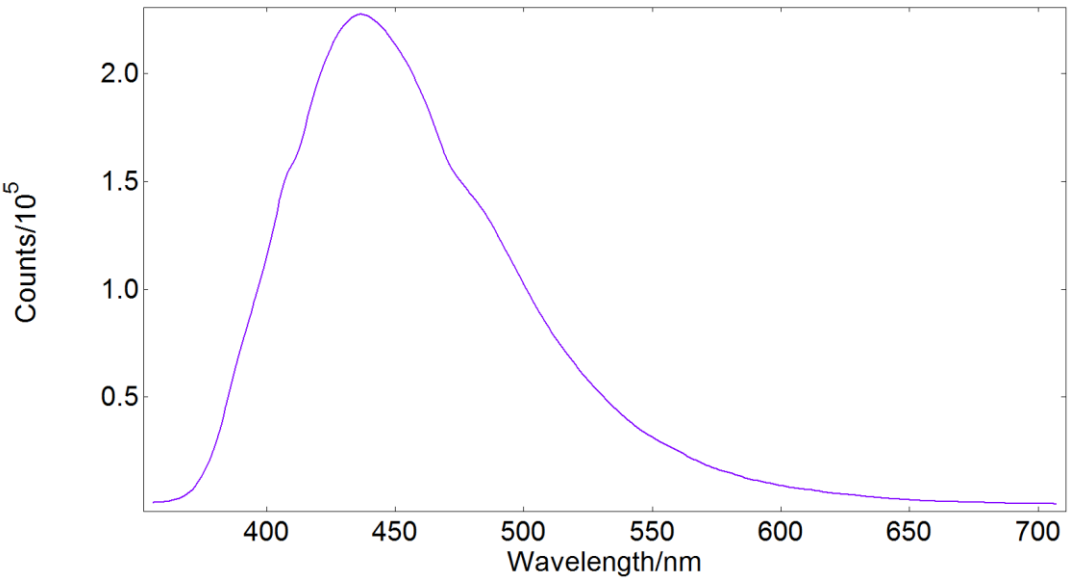

Fig. S18. Emission of **4b** in the solid state

In repeated measurements under the same experimental conditions (excitation source, wavelength, batch of the material, experimental setup) the Φ values of solid state luminophores **1**–**4** did not differ by more than 2% of the Φ value given in Table 1 (see manuscript). Accordingly, four repeated measurements for each compound were conducted (see below). The standard deviation (σ) for the measurements is within the expected range and would be fully obscured by the marker of each point in Figure 4C (see manuscript).

Table S1. Repeated measurements of solid state Φ for compounds **1**–**4**.

Compound	Φ_1, %	Φ_2, %	Φ_3, %	Φ_4, %	σ, %
1	16.9	17.2	17.1	17.7	0.3
2a	43.0	42.6	44.9	43.3	1.0
2b	34.9	34.3	35.8	35.1	0.6
3	83.6	87.0	84.9	85.2	1.4
4a	42.8	41.7	43.3	41.4	0.9
4b	18.5	19.7	18.8	19.3	0.5

X-Ray Structure, crystal data and structure refinements for 2a

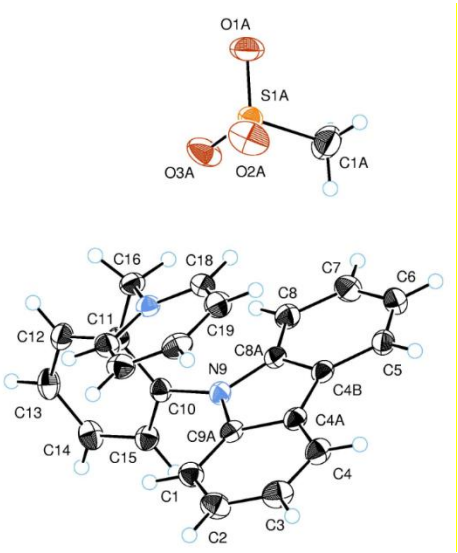

Identification code	KL-1291
Empirical formula	$C_{25}H_{22}N_2O_3S$
Formula weight	430.53
Temperature/K	150.0(1)
Crystal system	monoclinic
Space group	$P2_1/c$
a/Å	14.9750(1)
b/Å	19.7881(1)
c/Å	14.8102(1)
α/°	90
β/°	108.774(1)
γ/°	90
Volume/Å^3	4155.16(5)
Z	8
ρ_{calc}g/cm^3	1.3763
μ/mm^{-1}	1.635
F(000)	1808
Crystal size/mm^3	0.22 × 0.13 × 0.02
Radiation	Cu Kα (λ = 1.54184)
2Θ max. for data collection/°	155.0
Index ranges	$-18 \leq h \leq 18$, $-25 \leq k \leq 24$, $-18 \leq l \leq 17$
Reflections collected	63395
Independent reflections	8742 [R_{int} = 0.0391, R_{sigma} = 0.0231]
Data/restraints/parameters	8742/0/561
Goodness-of-fit on F^2	1.049
Final R indexes [$I \geq 2\sigma(I)$]	R_1 = 0.0378, wR_2 = 0.1005
Largest diff. peak/hole / e Å^{-3}	0.38/-0.48

X-Ray Structure, crystal data and structure refinements for 2b

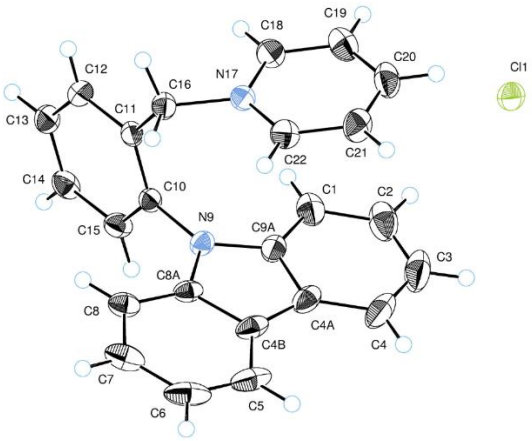

Identification code	KL1321
Empirical formula	$C_{24}H_{19}ClN_2$
Formula weight	370.86
Temperature/K	150.0(1)
Crystal system	monoclinic
Space group	$P2_1/c$
a/Å	8.90415(9)
b/Å	28.9401(2)
c/Å	7.98398(8)
α/°	90
β/°	111.1157(11)
γ/°	90
Volume/Å^3	1919.22(3)
Z	4
ρ_{calc}g/cm^3	1.283
μ/mm^{-1}	1.825
Crystal size/mm^3	0.21×0.17×0.06
Radiation	CuKα (λ = 1.54184)
2Θ max. for data collection/°	155.0
Reflections collected	24065
Independent reflections	4073
Restraints/parameters	0/245
Goodness-of-fit on F^2	1.054
Final *R* indexes [$I > 2\sigma(I)$]	R_1 = 0.0335, wR_2 = 0.0876
Final *R* indexes [all data]	R_1 = 0.0341, wR_2 = 0.0880
Largest diff. peak/hole / e Å^{-3}	0.26/-0.23

X-Ray Structure, crystal data and structure refinements for 3

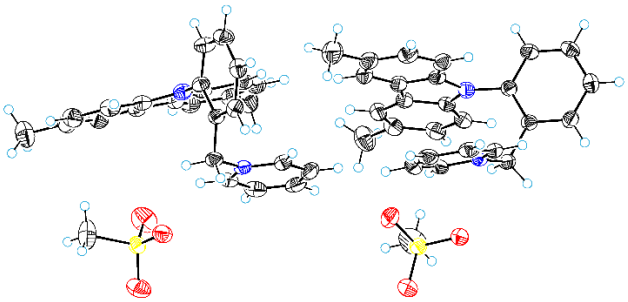

Identification code	KL-1421A
Empirical formula	$C_{54}H_{52}N_4O_6S_2$
Formula weight	917.17
Temperature/K	150.0(3)
Crystal system	triclinic
Space group	$P\ \bar{1}$
a/Å	13.3101(3)
b/Å	13.4723(5)
c/Å	13.9252(3)
α/°	101.733(3)
β/°	102.111(2)
γ/°	100.527(3)
Volume/Å^3	2323.25(12)
Z	2
ρ_{calc}g/cm^3	1.3110
μ/mm^{-1}	1.493
Crystal size/mm^3	0.19 × 0.06 × 0.01
Radiation	CuKα (λ = 1.54184)
2Θ max. for data collection/°	160.0
Reflections collected	12221
Independent reflections	9928
Restraints/parameters	0/601
Goodness-of-fit on F^2	1.196
Final *R* indexes [$I > 2\sigma(I)$]	R_1 = 0.0953, wR_2 = 0.2903
Final *R* indexes [all data]	R_1 = 0.1046, wR_2 = 0.2957
Largest diff. peak/hole / e Å^{-3}	1.97/-0.70

X-Ray Structure, crystal data and structure refinements for 4a

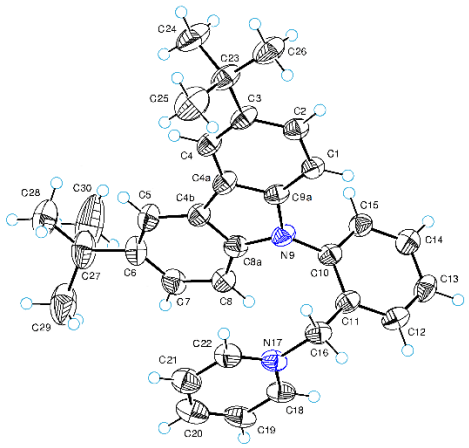

Identification code	kl1418
Empirical formula	$C_{64}H_{70}Cl_2N_4$
Formula weight	966.14
Temperature/K	150.0(2)
Crystal system	monoclinic
Space group	$P2_1/n$
a/Å	10.2702(7)
b/Å	12.6758(9)
c/Å	41.470(3)
α/°	90
β/°	90.17(1)
γ/°	90
Volume/Å^3	5398.7(7)
Z	4
ρ_{calc}g/cm^3	1.189
μ/mm^{-1}	1.406
Crystal size/mm^3	0.22 × 0.12 × 0.03
Radiation	CuKα (λ = 1.54184)
2Θ max. for data collection/°	160.0
Reflections collected	15044
Independent reflections	10487
Restraints/parameters	0/655
Goodness-of-fit on F^2	1.110
Final *R* indexes [$I > 2\sigma(I)$]	R_1 = 0.1247, wR_2 = 0.3594
Final *R* indexes [all data]	R_1 = 0.1406, wR_2 = 0.3701
Largest diff. peak/hole / e Å^{-3}	1.39/-0.54

X-Ray Structure, crystal data and structure refinements for 4b

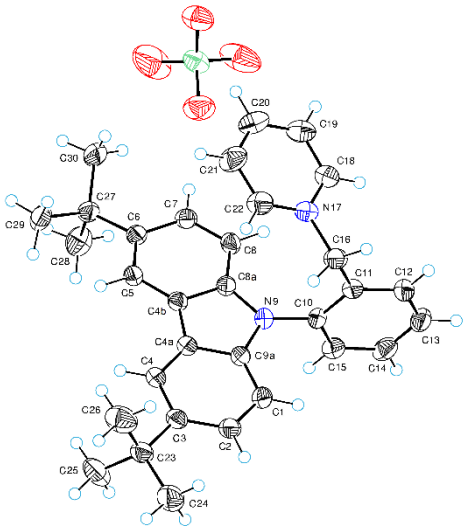

Identification code	C1418
Empirical formula	$C_{32}H_{35}ClN_2O_4$
Formula weight	547.10
Temperature/K	150.0(1)
Crystal system	orthorhombic
Space group	*Pbca*
a/Å	12.1430(4)
b/Å	11.0905(4)
c/Å	42.6477(15)
α/°	90
β/°	90
γ/°	90
Volume/Å^3	5743.4(4)
Z	8
ρ_{calc}g/cm^3	1.2653
μ/mm^{-1}	1.491
Crystal size/mm^3	0.17 × 0.16 × 0.01
Radiation	Cu Kα (λ = 1.54184 Å)
2Θ max. for data collection/°	160.0
Reflections collected	30498
Independent reflections	6185
Restraints/parameters	0/358
Goodness-of-fit on F^2	1.060
Final *R* indexes [$I > 2\sigma(I)$]	R_1 = 0.0664, wR_2 = 0.1566
Final *R* indexes [all data]	R_1 = 0.0859, wR_2 = 0.1670
Largest diff. peak/hole / e Å^{-3}	0.55/-0.45

Quantum chemical calculations

Charge transfer integral calculations

Every considered charge transfer (CT) pathway for 1–4

Geometries of the molecules were obtained from the X-Ray analysis data.

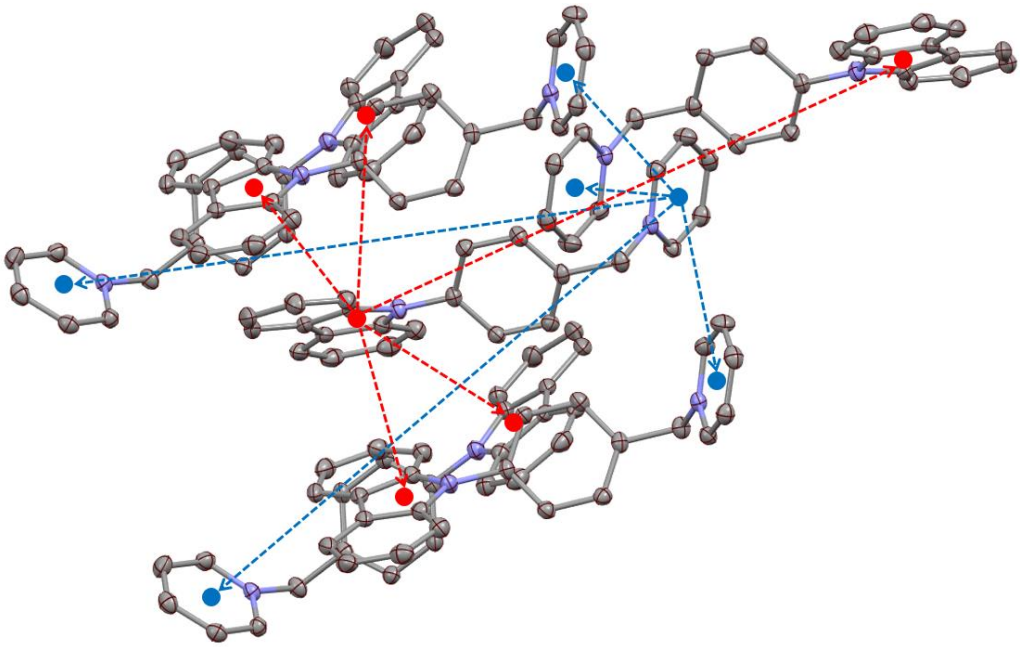

Fig. S19. Every electron (blue vectors) and hole (red vectors) CT pathway considered for **1**

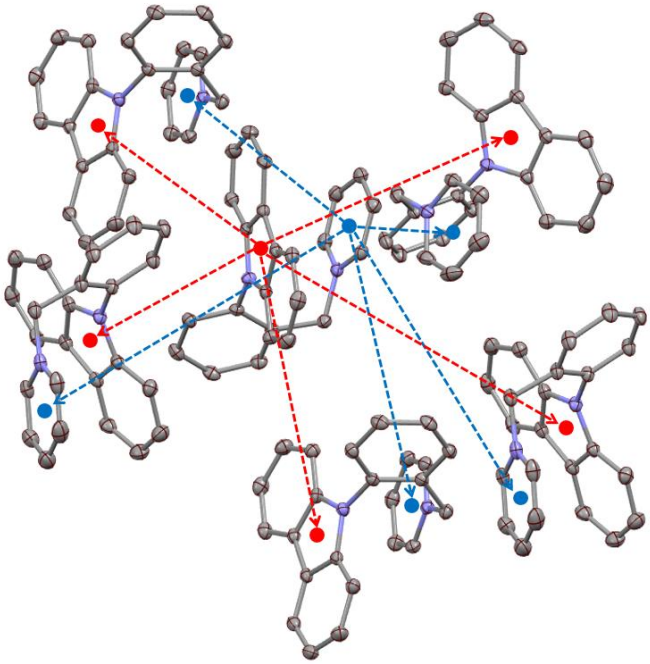

Fig. S20. Every electron (blue vectors) and hole (red vectors) CT pathway considered for **2a**

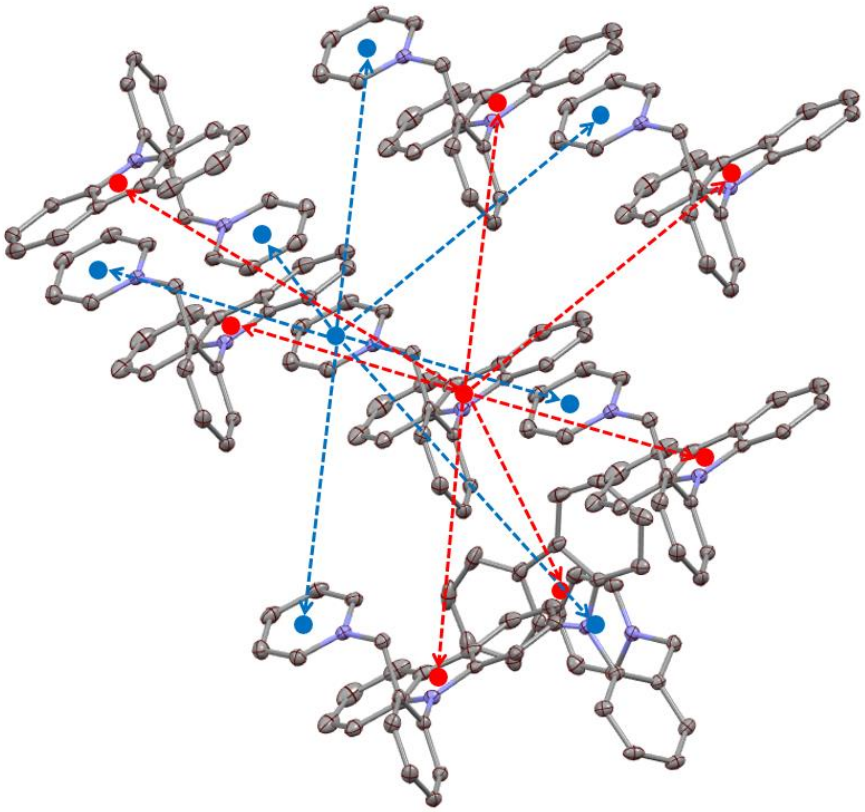

Fig. S21. Every electron (blue vectors) and hole (red vectors) CT pathway considered for **2b**

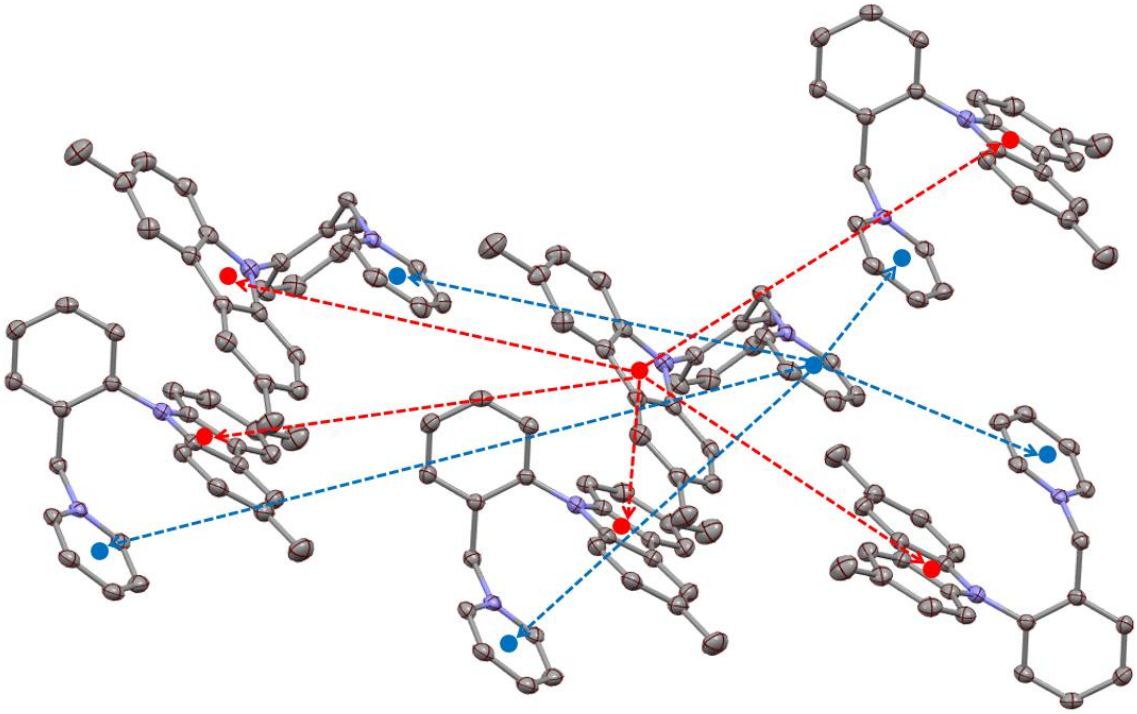

Fig. S22. Every electron (blue vectors) and hole (red vectors) CT pathway considered for **3**

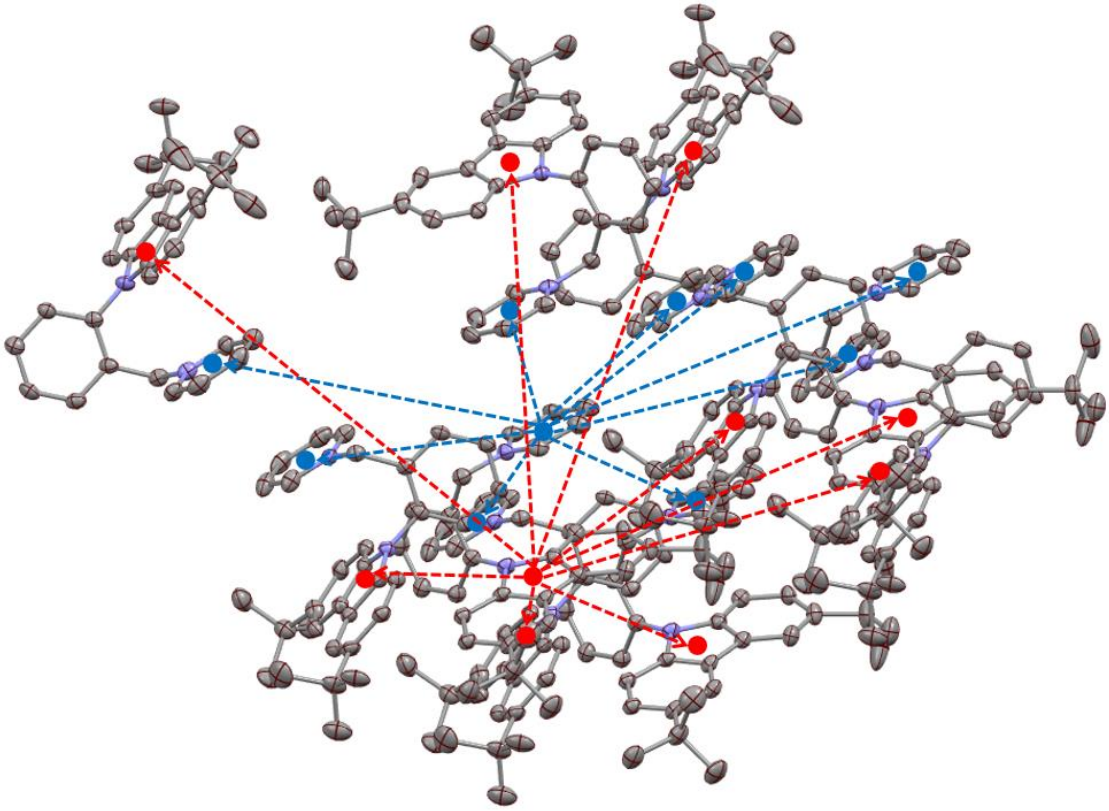

Fig. S23. Every electron (blue vectors) and hole (red vectors) CT pathway considered for **4a**

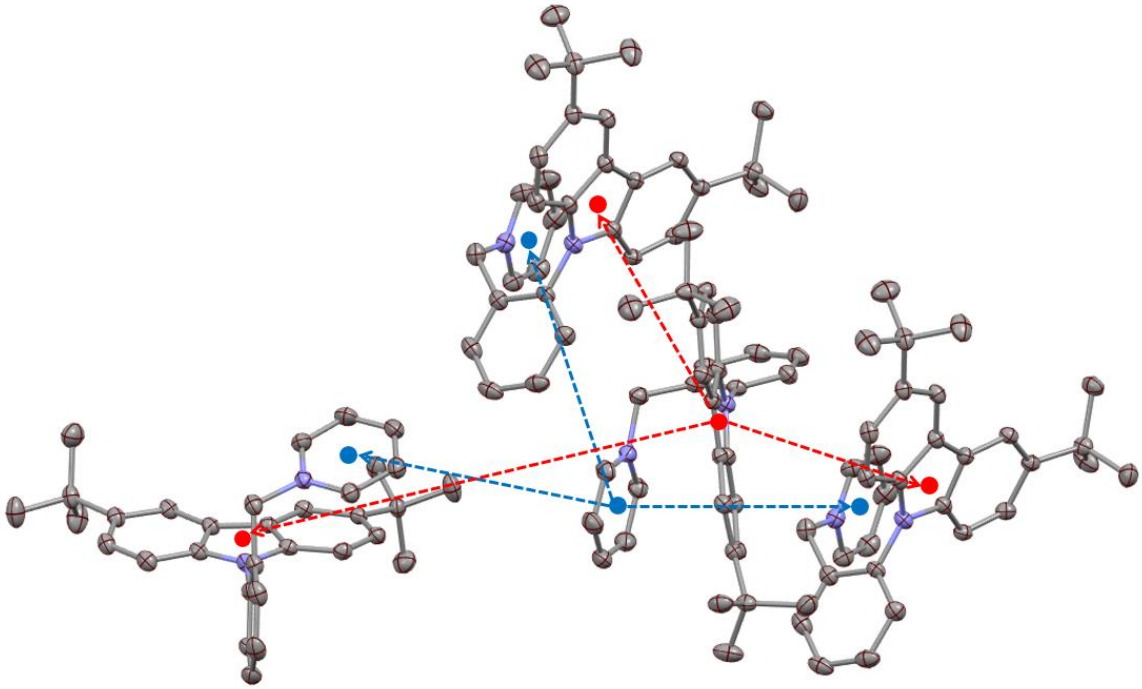

Fig. S24. Every electron (blue vectors) and hole (red vectors) CT pathway considered for **4b**

Calculation methodology for electronic coupling:

Luminophore molecules in their corresponding geometries were obtained from the X-ray analysis data. The geometries of dimers were obtained by selecting short contacts from X-ray analysis data. Only unique geometries of the short contact pairs were used in further calculations without additional geometry optimization. For each pair of the dimers HOMO and LUMO data of dimer and individual monomers were calculated. CTIs were calculated for both electron transfer (LUMO, blue vectors, $E_{1–3}$) and hole transfer (HOMO, red vectors, $H_{1–3}$) using CATNIP (Brown, J. S. Catnip (version 1.9), **2018** software. (Available from https://github.com/JoshuaSBrown/QC_Tools) For all CT pathways in compounds **1**–**4** the absolute value of electronic coupling (|V|) was claculated using dimers of the corresponding compound. Their absolute hole (HOMO-HOMO) and electron (LUMO-LUMO) coupling values were calculated using formula:

$$|V| = |\frac{J - S(\varepsilon_1 + \varepsilon_2)}{1 - S^2}|,$$

where

J – charge transfer integral; ε_1 – site energy for 1st luminophore of the chosen dimer; ε_2 – site energy for 2nd luminophore for the chosen dimer; S – overlap integral.

The calculations for HOMOs and LUMOs were performed using Gaussian 09[3] software using B3LYP/6-311++g(2df,p) level of theory. The use of CAM-B3LYP/6-311++g(2df,p) basis set afforded similar results.

Hardware for calculations: the cluster for calculations consisted of: 2x Intel Xeon E5-2630 v2 (6 cores)/64 GB RAM/2x Nvidia Tesla K20M nodes. The calculations were performed on 10 cores with 50 GB RAM. The longest CPU time for a single dimer was 2d 1h 51min 20.2s.

For simplicity, the number of charge transfer pathways for each compound were limited to three hole and three electron pathways with the highest |V| value. The disregarded pathways contributed less than 3% of the total sum of |V| (Σ|V|).

Data of the hole and electron CT pathways for luminophores 1–4

H_n – hole transfer pathways, n = 1–3; E_n – electron transfer pathways, n = 1–3

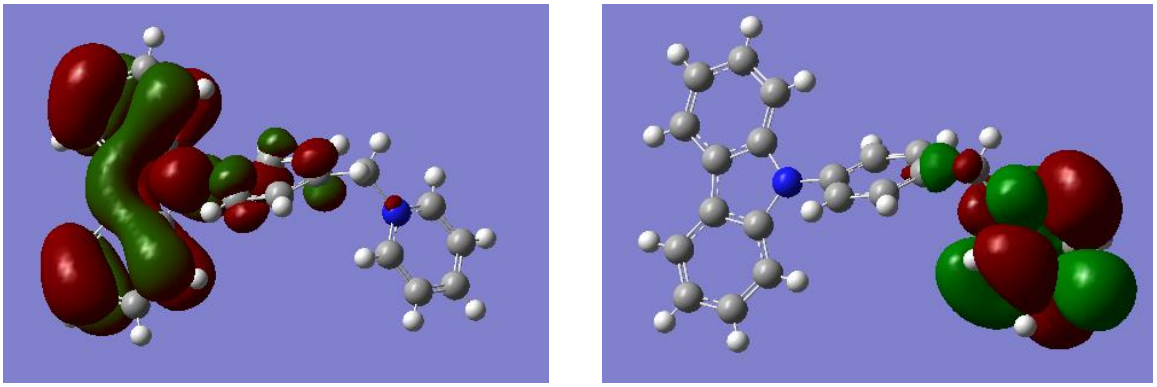

HOMO LUMO

Fig. S25. Representation of HOMO and LUMO orbitals of compound **1**

Table S2. Electron coupling and energy calculation results for emitter **1**

		H_1	H_2	H_3
HOMO-HOMO, Hole transfer	**J**	-0.0099	0.0516	0.0380
	ε_1	-9.6448	-9.4751	-9.1907
	ε_2	-9.6446	-9.1446	-9.2187
	S	0.0006	-0.0034	-0.0033
	|V|, eV	0.0042	0.0204	0.0077
$E_{(RB3LYP)}$, A.U.		-2070.388	-2070.433	-2070.401

		E_1	E_2	E_3
LUMO-LUMO, Electron transfer	**J**	0.1388	0.0006	-0.0048
	ε_1	-8.8727	-7.6458	-8.2709
	ε_2	-8.8734	-7.5824	-8.2879
	S	-0.0101	-0.0001	0.0003
	|V|, eV	0.0494	0.0001	0.0023
$E_{(RB3LYP)}$, A.U.		-2070.388	-2070.433	-2070.401

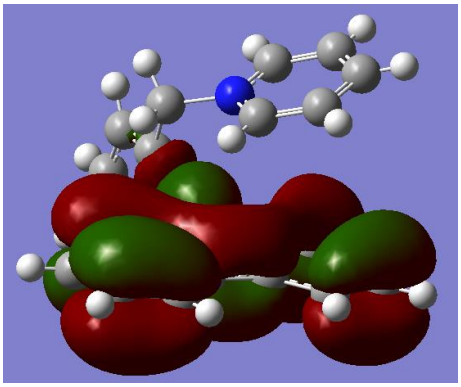

HOMO

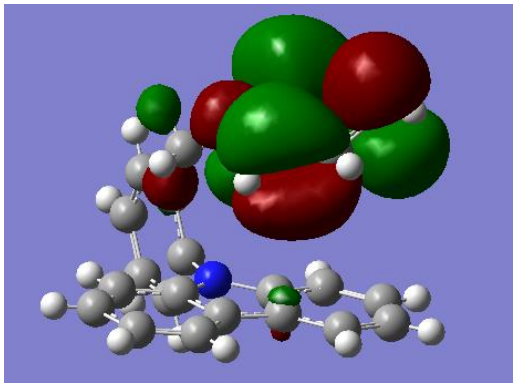

LUMO

Fig. S26. Representation of HOMO and LUMO orbitals of compound **2a**

Table S3. Electron coupling and energy calculation results for emitter **2a**

		H_1	**H_2**	**H_3**
HOMO-HOMO, Hole transfer	**J**	-0.0036	0.0722	-0.0085
	ε_1	-10.0517	-10.3287	-10.2146
	ε_2	-10.4751	-10.4134	-9.8416
	S	0.0001	-0.0047	0.0007
	|V|, eV	0.0023	0.0236	0.0017
$E_{(RB3LYP)}$, A.U.		-2070.420	-2070.432	-2070.437

		E_1	**E_2**	**E_3**
LUMO-LUMO, Electron transfer	**J**	0.0110	-0.2184	-0.0001
	ε_1	-7.9428	-8.5041	-7.6042
	ε_2	-7.8967	-8.4500	-7.5108
	S	-0.0009	0.0154	0.00001
	|V|, eV	0.0036	0.0877	0.00002
$E_{(RB3LYP)}$, A.U.		-2070.420	-2070.401	-2070.437

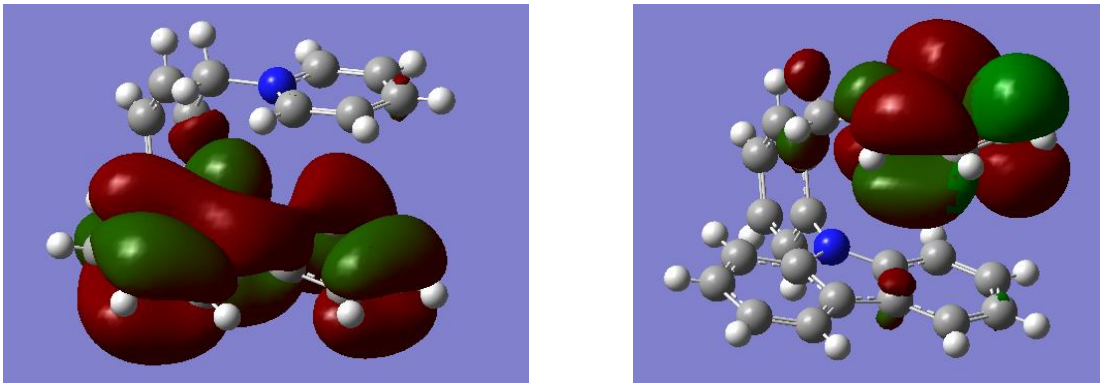

HOMO LUMO

Fig. S27. Representation of HOMO and LUMO orbitals of compound **2b**

Table S4. Electron coupling and energy calculation results for emitter **2b**

		H_1	H_2	H_3
HOMO-HOMO, Hole transfer	**J**	0.0124	0.1001	-0.0328
	ε_1	-10.0573	-10.0815	-10.0345
	ε_2	-9.9387	-10.1741	-10.2457
	S	-0.0008	-0.0070	0.0021
	|V|, eV	0.0043	0.0289	0.0113
$E_{(RB3LYP)}$, A.U.		-2070.428	-2070.436	-2070.419

		E_1	E_2	E_3
LUMO-LUMO, Electron transfer	**J**	-0.0863	-0.0552	0.0180
	ε_1	-8.4170	-7.8138	-7.7625
	ε_2	-8.4167	-7.8140	-7.6842
	S	0.0053	0.0048	-0.0016
	|V|, eV	0.0413	0.0174	0.0055
$E_{(RB3LYP)}$, A.U.		-2070.400	-2070.415	-2070.419

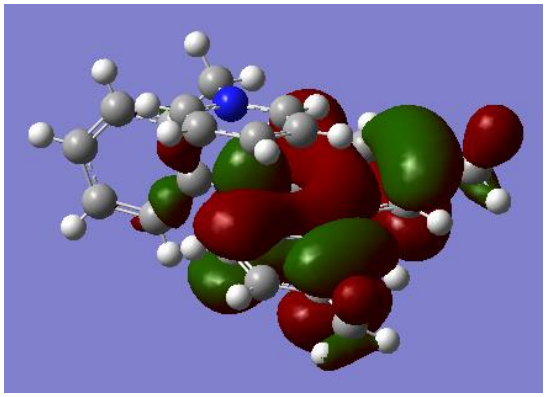

HOMO

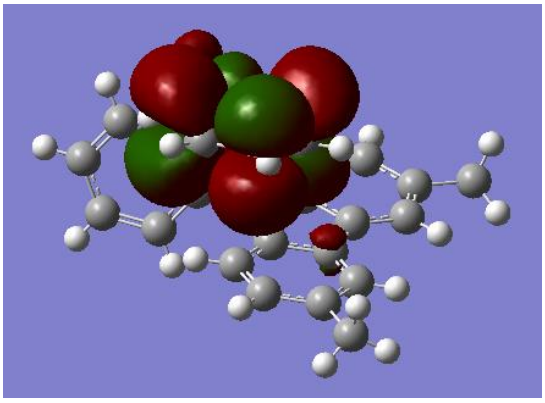

LUMO

Fig. S28. Representation of HOMO and LUMO orbitals of compound **3**

Table S5. Electron coupling and energy calculation results for emitter **3**

		H_1	H_2	H_3
HOMO-HOMO, Hole transfer	**J**	-0.0028	0.0083	0.0116
	ε_1	-9.9012	-10.2161	-9.6254
	ε_2	-9.8988	-9.6118	-10.1842
	S	0.0002	-0.0006	-0.0008
	|V|, eV	0.0011	0.0022	0.0032
$E_{(RB3LYP)}$, A.U.		-2227.860	-2227.874	-2227.874

		E_1	E_2	E_3
LUMO-LUMO, Electron transfer	**J**	-0.7927	-0.0079	-0.0137
	ε_1	-8.3375	-7.5282	-7.7939
	ε_2	-8.3346	-7.5165	-7.9365
	S	0.0613	0.0007	0.0014
	|V|, eV	0.2829	0.0025	0.0029
$E_{(RB3LYP)}$, A.U.		-2227.860	-2227.886	-2227.874

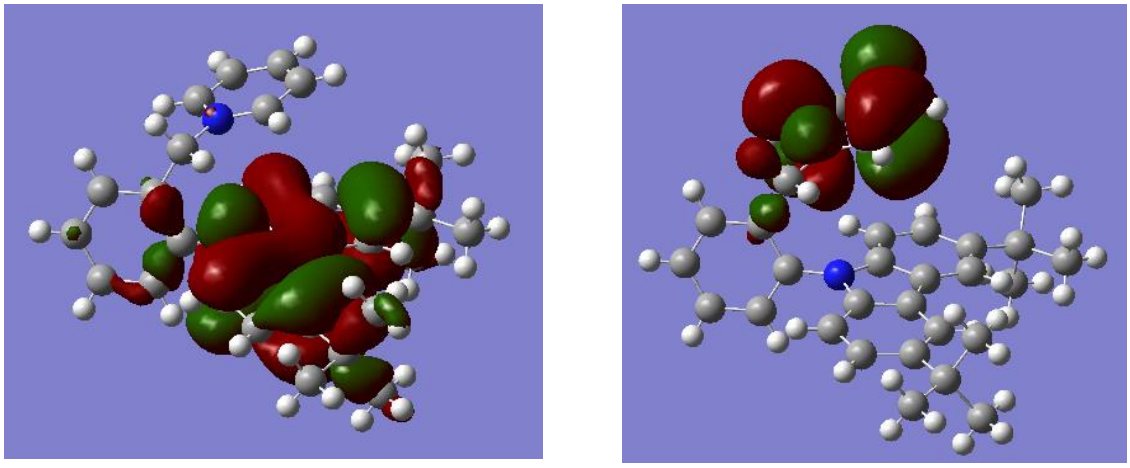

HOMO LUMO

Fig. S29. Representation of HOMO and LUMO orbitals of compound **4a**

Table S6. Electron coupling and energy calculation results for emitter **4a**

		H_1	**H_2**	**H_3**
HOMO-HOMO, Hole transfer	**J**	0.0784	0.0557	0.0220
	ε_1	-9.7809	-9.7064	-9.2895
	ε_2	-9.7401	-9.7946	-9.3578
	S	-0.0049	-0.0036	-0.0016
	|V|, eV	0.0307	0.0211	0.0075
$E_{(RB3LYP)}$, A.U.		-2699.503	-2699.504	-2699.525

		E_1	**E_2**	**E_3**
LUMO-LUMO, Electron transfer	**J**	-0.1029	0.0780	0.0867
	ε_1	-8.3346	-8.0736	-7.9269
	ε_2	-8.3275	-7.9298	-8.1118
	S	0.0075	-0.0063	-0.0069
	|V|, eV	0.0403	0.0277	0.0317
$E_{(RB3LYP)}$, A.U.		-2699.500	-2699.503	-2699.504

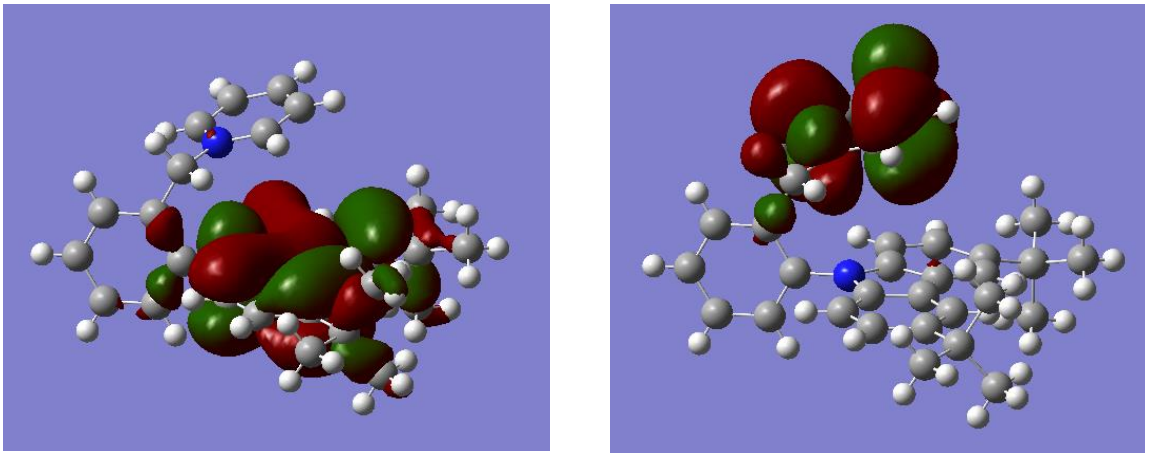

HOMO LUMO

Fig. S30. Representation of HOMO and LUMO orbitals of compound **4b**

Table S7. Electron coupling and energy calculation results for emitter **4b**

		H_1	H_2	H_3
HOMO-HOMO, Hole transfer	**J**	0.0847	-0.0007	-0.0047
	ε_1	-9.6548	-9.3320	-9.2602
	ε_2	-9.8017	-9.3164	-9.3233
	S	-0.0054	0.0001	0.0003
	|V|, eV	0.0326	0.0003	0.0015
$E_{(RB3LYP)}$, A.U.		-2699.532	-2699.541	-2699.554

		E_1	E_2	E_3
LUMO-LUMO, Electron transfer	**J**	0.0756	0.0495	-0.0021
	ε_1	-7.8299	-7.6996	-7.4270
	ε_2	-7.9884	-7.8597	-7.4719
	S	-0.0066	-0.0043	0.0002
	|V|, eV	0.0237	0.0159	0.0008
$E_{(RB3LYP)}$, A.U.		-2699.532	-2699.541	-2699.554

Accordingly, the CTI analysis demonstrated that the sum of absolute electronic couplings Σ(|V|) for each of the luminophores **1**–**4** correlated well (R^2=0.95) with the corresponding solid state Φ (see manuscript for details).

CTI analysis for luminophores 15–17

CTI analysis (as described above) was also performed for luminophores **15**–**17** of completely distinct design, developed in 2020 by Shi, Lu and co-workers[4] (Fig. S31).

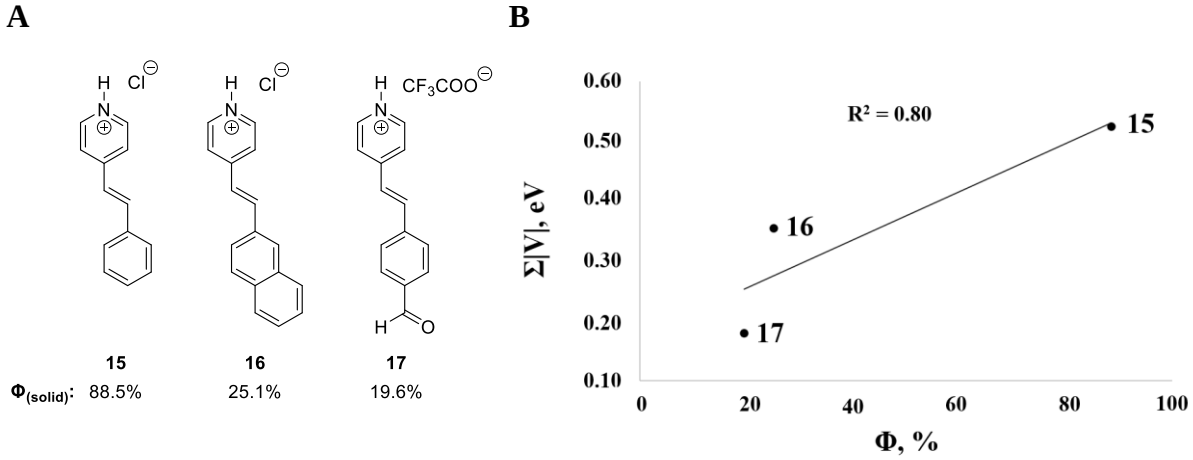

Fig. S31. A: Luminophores **15**–**17**; B: Correlation between the Σ|V| and Φ for **15**–**17**

Table S8. Electron coupling and energy calculation results for emitter **15**

		H_1	H_2	H_3
HOMO-HOMO, Hole transfer	**J**	-0.4088	0.0005	0.4140
	ε_1	-12.3148	-11.1400	-12.1624
	ε_2	-12.3154	-11.3729	-12.1624
	S	0.0220	-0.0000	-0.0228
	|V|, eV	0.1386	0.0003	0.1373
$E_{(RB3LYP)}$, A.U.		-1113.994	-1114.002	-1114.001

		E_1	E_2	E_3
LUMO-LUMO, Electron transfer	**J**	0.1894	-0.0145	-0.3810
	ε_1	-8.8479	-8.1884	-8.6213
	ε_2	-8.8471	-8.3241	-8.6213
	S	-0.0123	0.0014	0.0252
	|V|, eV	0.0809	0.0030	0.1641
$E_{(RB3LYP)}$, A.U.		-1113.994	-1114.002	-1114.001

Table S9. Electron coupling and energy calculation results for emitter **16**

		H_1	H_2	H_3
HOMO-HOMO, Hole transfer	**J**	-0.0023	-0.4172	-0.0098
	ε_1	-10.0394	-11.1654	-9.8120
	ε_2	-10.0399	-11.1631	-9.8109
	S	0.0004	0.0244	0.0008
	|V|, eV	0.0014	0.1449	0.0018
$E_{(RB3LYP)}$, A.U.		-1421.344	-1421.315	-1421.351

		E_1	E_2	E_3
LUMO-LUMO, Electron transfer	**J**	-0.4534	0.0021	0.0244
	ε_1	-8.5060	-7.8924	-8.0894
	ε_2	-8.5066	-7.6158	-8.0905
	S	0.0296	-0.0002	-0.0025
	|V|, eV	0.2016	0.0005	0.0043
$E_{(RB3LYP)}$, A.U.		-1421.315	-1421.338	-1421.320

Table S10. Electron coupling and energy calculation results for emitter **17**

		H_1	H_2	H_3
HOMO-HOMO, Hole transfer	**J**	-0.0173	0.0070	0.0020
	ε_1	-11.9185	-11.1882	-11.8367
	ε_2	-11.9191	-11.1882	-10.5221
	S	0.0010	-0.0004	-0.0002
	|V|, eV	0.0049	0.0021	0.0003
$E_{(RB3LYP)}$, A.U.		-1340.788	-1340.774	-1340.759

		E_1	E_2	E_3
LUMO-LUMO, Electron transfer	**J**	-0.4227	0.0072	-0.0071
	ε_1	-9.1968	-8.0516	-8.5747
	ε_2	-9.1971	-8.0512	-8.0043
	S	0.0281	-0.0005	0.0004
	|V|, eV	0.1646	0.0033	0.0037
$E_{(RB3LYP)}$, A.U.		-1340.728	-1340.788	-1340.759

The CTI analysis demonstrated that the sum of absolute electronic couplings Σ(|V|) for luminophores **15**–**17** correlated well with the corresponding solid state Φ values. The lower correlation value (R^2=0.80) for **15**–**17** as compared to that for luminophores **1**–**4** possibly is a consequence of insufficient data points (only three are available) and overestimation of the CTI value for **16**, due to the larger total π-system of the molecule.

References

1. K. Leduskrasts, E. Suna, *RSC Adv.* **2019**, *9*, 460–465. DOI: 10.1039/C8RA08771G
2. Brown, J. S. Catnip (version 1.9), **2018**. Available from https://github.com/JoshuaSBrown/QC_Tools
3. Frisch, M. J.; Trucks, G. W.; Schlegel, H. B.; Scuseria, G. E.; Robb, M. A.; Cheeseman, J. R.; Scalmani, G.; Barone, V.; Mennucci, B.; Petersson, G. A.; Nakatsuji, H.; Caricato, M.; Li, X.; Hratchian, H. P.; Izmaylov, A. F.; Bloino, J.; Zheng, G.; Sonnenberg, J. L.; Hada, M.; Ehara, M.; Toyota, K.; Fukuda, R.; Hasegawa, J.; Ishida, M.; Nakajima, T.; Honda, Y.; Kitao, O.; Nakai, H.; Vreven, T.; Jr., J. A. M.; Peralta, J. E.; Ogliaro, F.; Bearpark, M.; Heyd, J. J.; Brothers, E.; Kudin, K. N.; Staroverov, V. N.; Keith, T.; Kobayashi, R.; Normand, J.; Raghavachari, K.; Rendell, A.; Burant, J. C.; Iyengar, S. S.; Tomasi, J.; Cossi, M.; Rega, N.; Millam, J. M.; Klene, M.; Knox, J. E.; Cross, J. B.; Bakken, V.; Adamo, C.; Jaramillo, J.; Gomperts, R.; Stratmann, R. E.; Yazyev, O.; Austin, A. J.; Cammi, R.; Pomelli, C.; Ochterski, J. W.; Martin, R. L.; Morokuma, K.; Zakrzewski, V. G.; Voth, G. A.; Salvador, P.; Dannenberg, J. J.; Dapprich, S.; Daniels, A. D.; Farkas, O.; Foresman, J. B.; Ortiz, J. V.; Cioslowski, J.; Fox, D. J. Gaussian 09, Revision D.01, 2013.
4. X. Cui, Y. Hao, W. Guan, L. Liu, W. Shi, C. Lu, *Adv. Opt. Mater.*, 2020, **8**, 2000125. DOI: 10.1002/adom.202000125

^{1}H and ^{13}C NMR data

^{1}H NMR (400 MHz, $(CD_3)_2SO$, ppm) spectrum of 1-(2-(9*H*-carbazol-9-yl)benzyl)pyridin-1-ium methanesulfonate (**2a**)

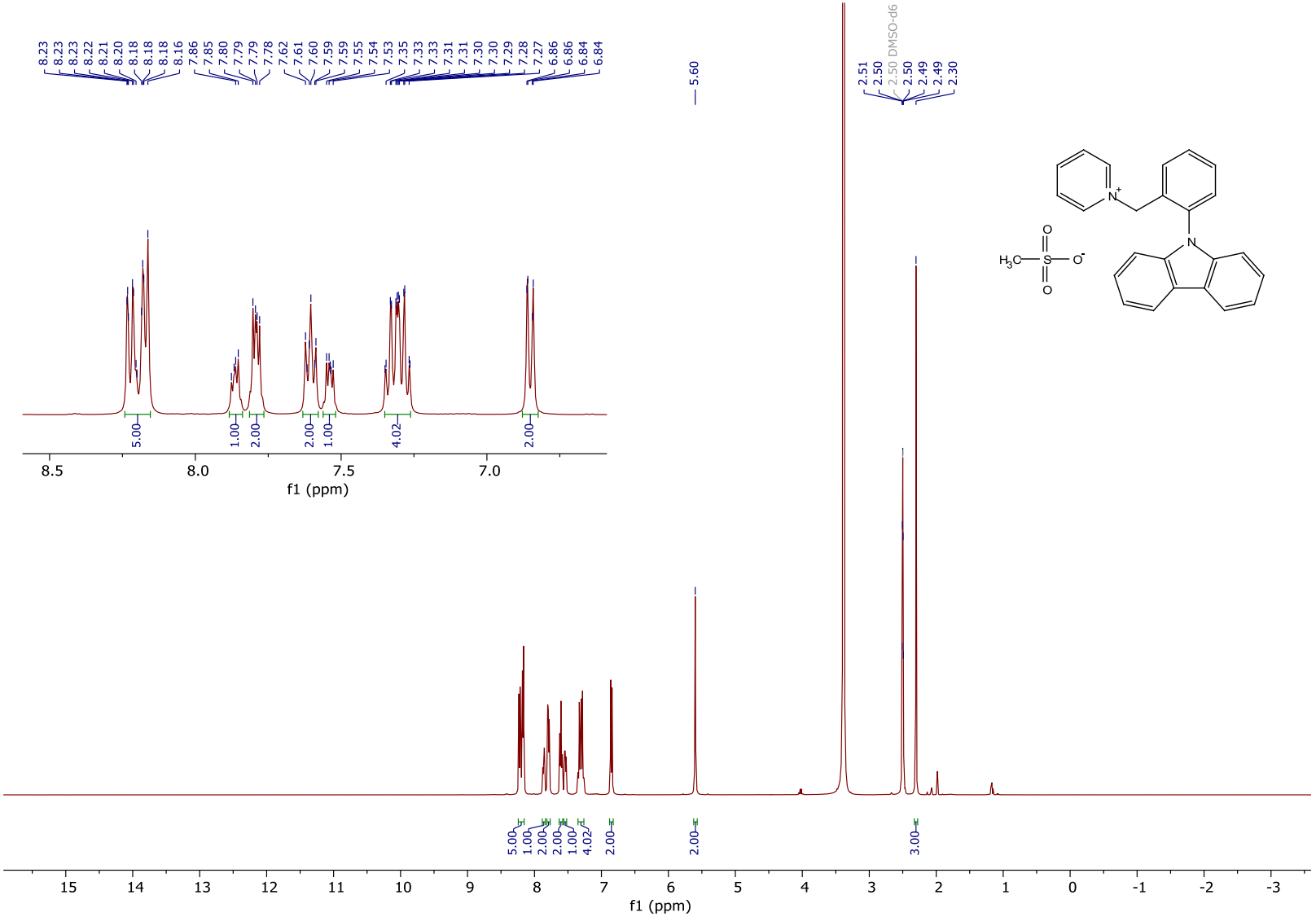

$^{13}C\{^{1}H\}$ NMR (101 MHz, $(CD_3)_2SO$, ppm) spectrum of 1-(2-(9*H*-carbazol-9-yl)benzyl)pyridin-1-ium methanesulfonate (**2a**)

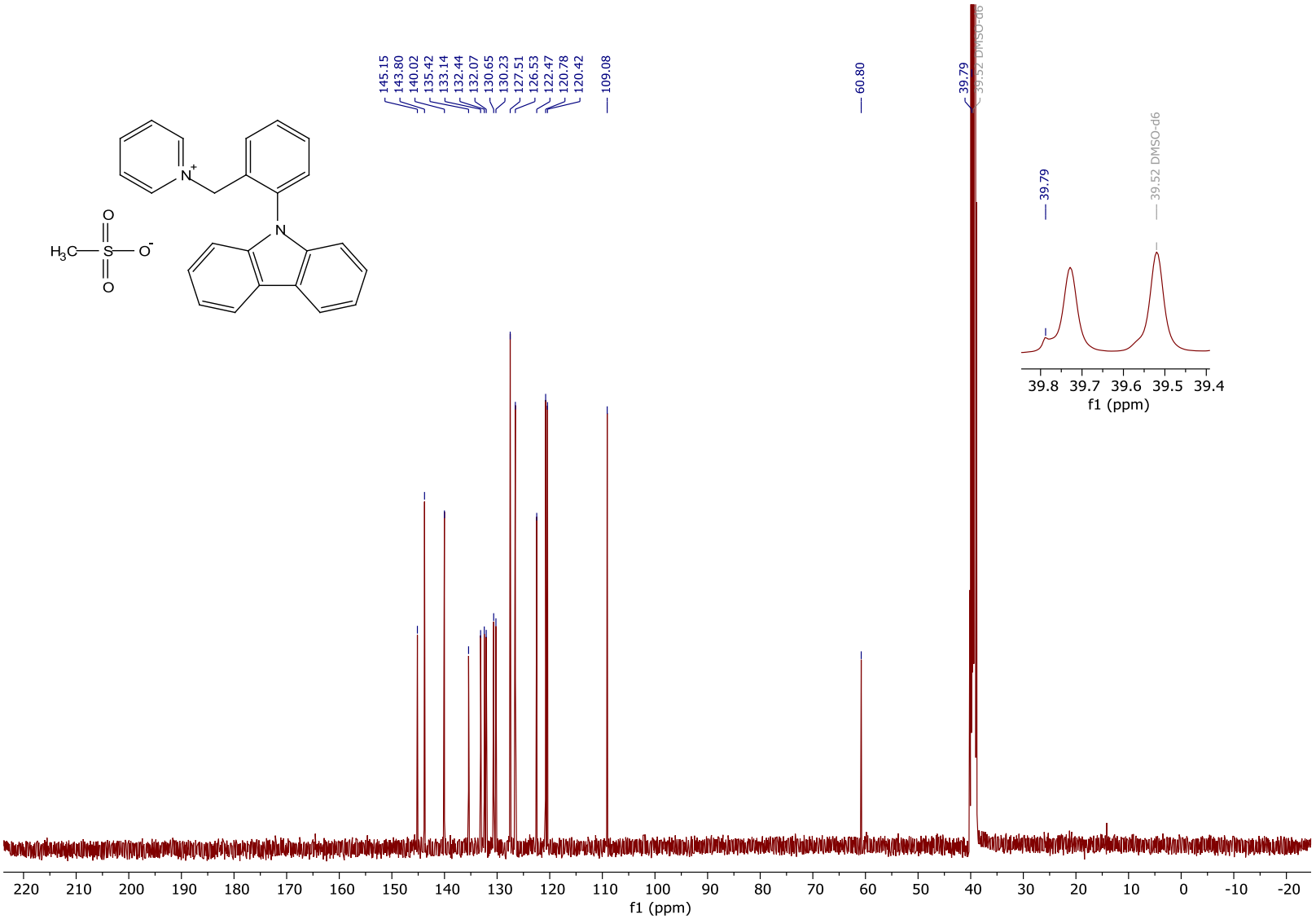

^{1}H NMR (400 MHz, $(CD_3)_2SO$, ppm) spectrum of 1-(2-(9*H*-carbazol-9-yl)benzyl)pyridin-1-ium chloride (**2b**)

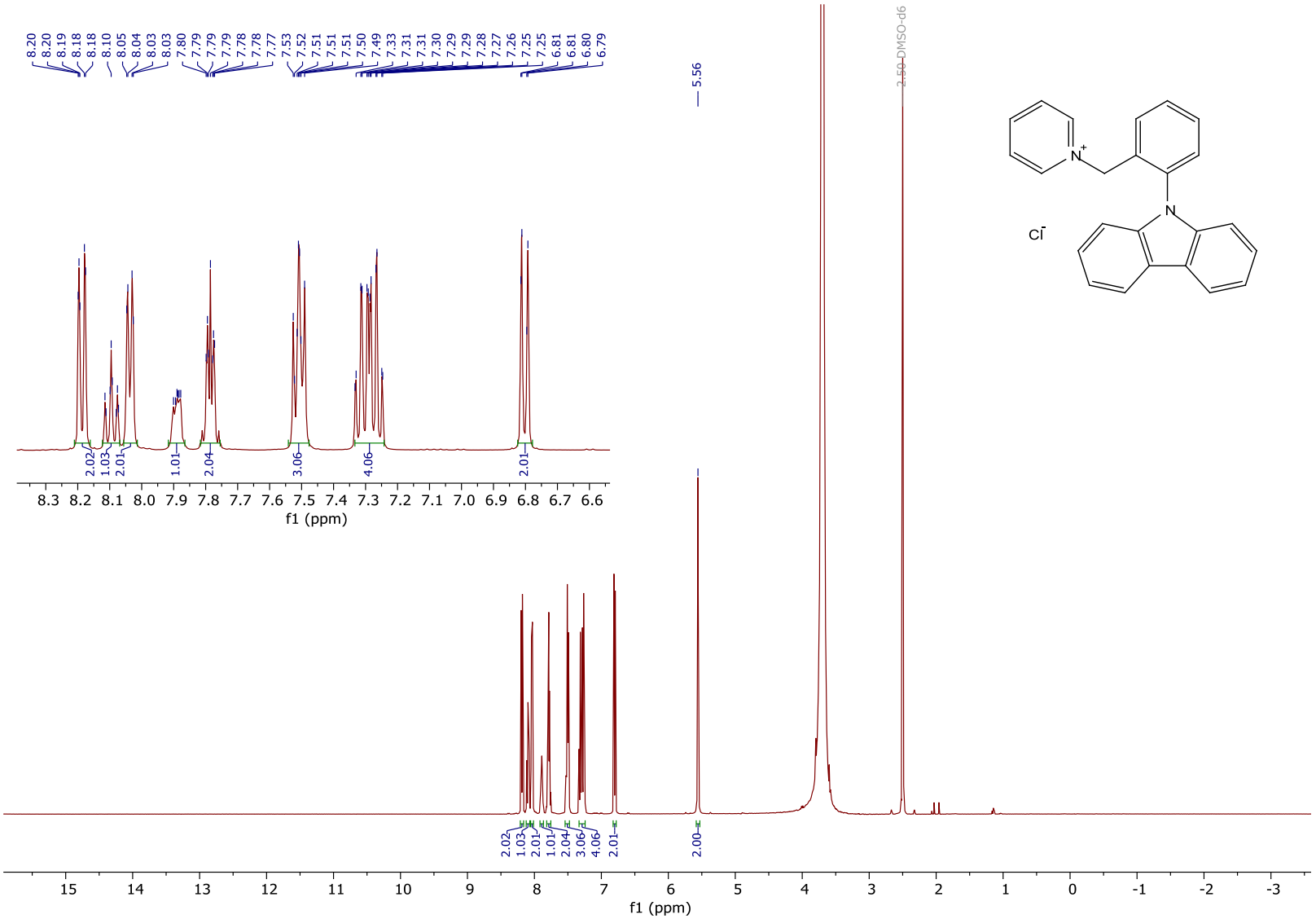

$^{13}C\{^{1}H\}$ NMR (101 MHz, $(CD_3)_2SO$, ppm) spectrum of 1-(2-(9*H*-carbazol-9-yl)benzyl)pyridin-1-ium chloride (**2b**)

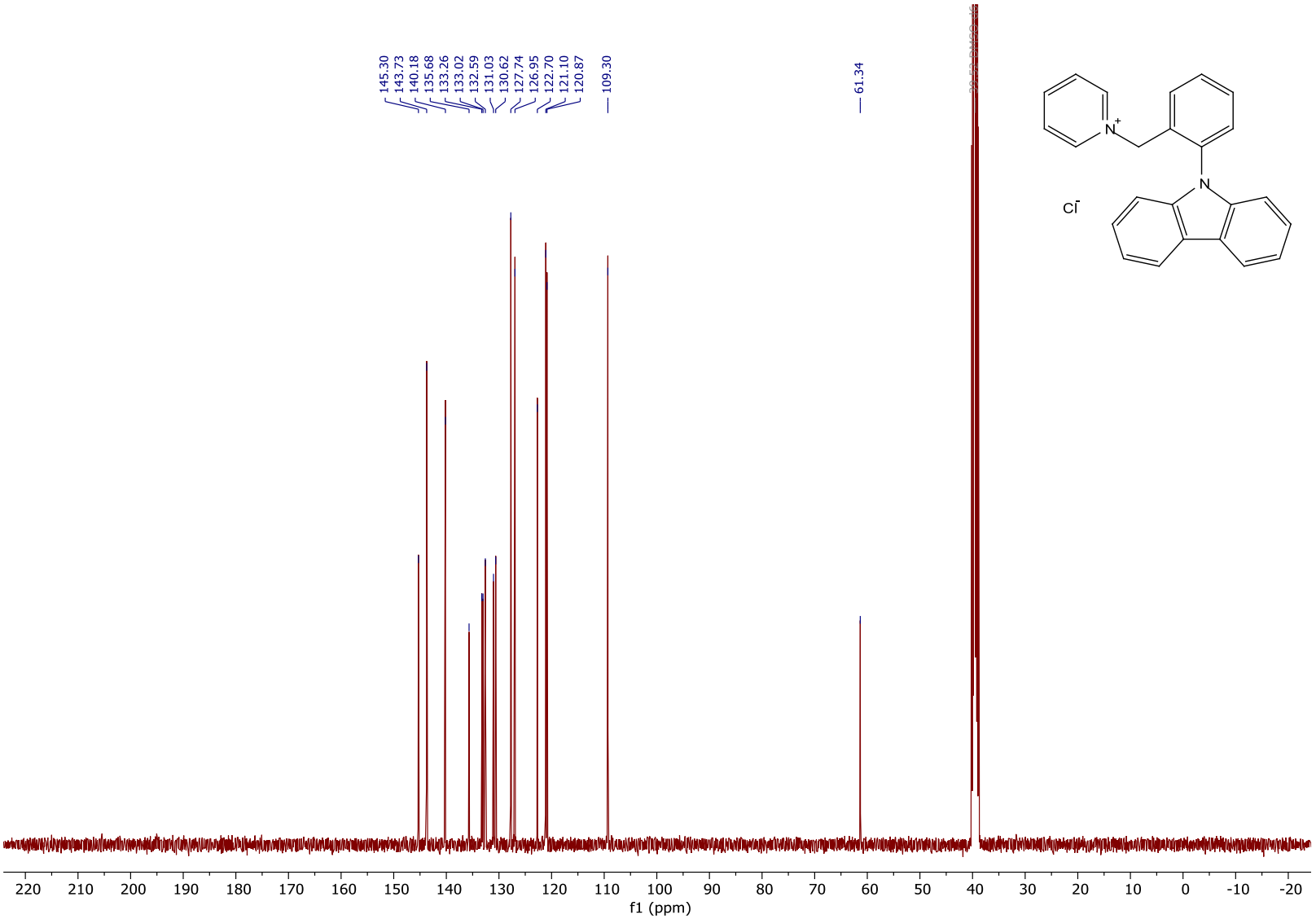

^{1}H NMR (400 MHz, CD_3OD, ppm) spectrum of 1-(2-(3,6-dimethyl-9*H*-carbazol-9-yl)benzyl)pyridin-1-ium methanesulfonate (**3**)

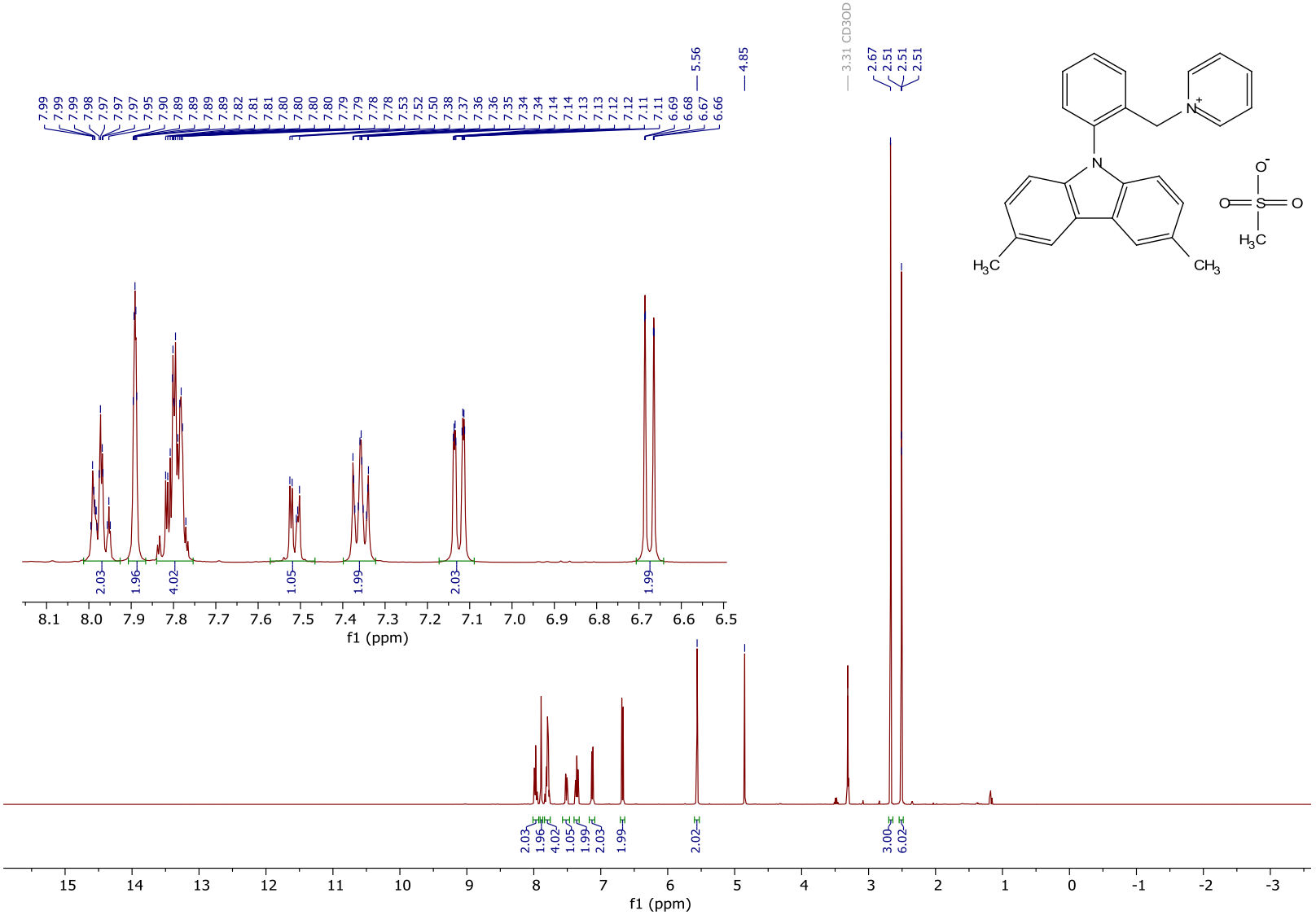

$^{13}C\{^{1}H\}$ NMR (101 MHz, CD_3OD, ppm) spectrum of 1-(2-(3,6-dimethyl-9*H*-carbazol-9-yl)benzyl)pyridin-1-ium methanesulfonate (**3**)

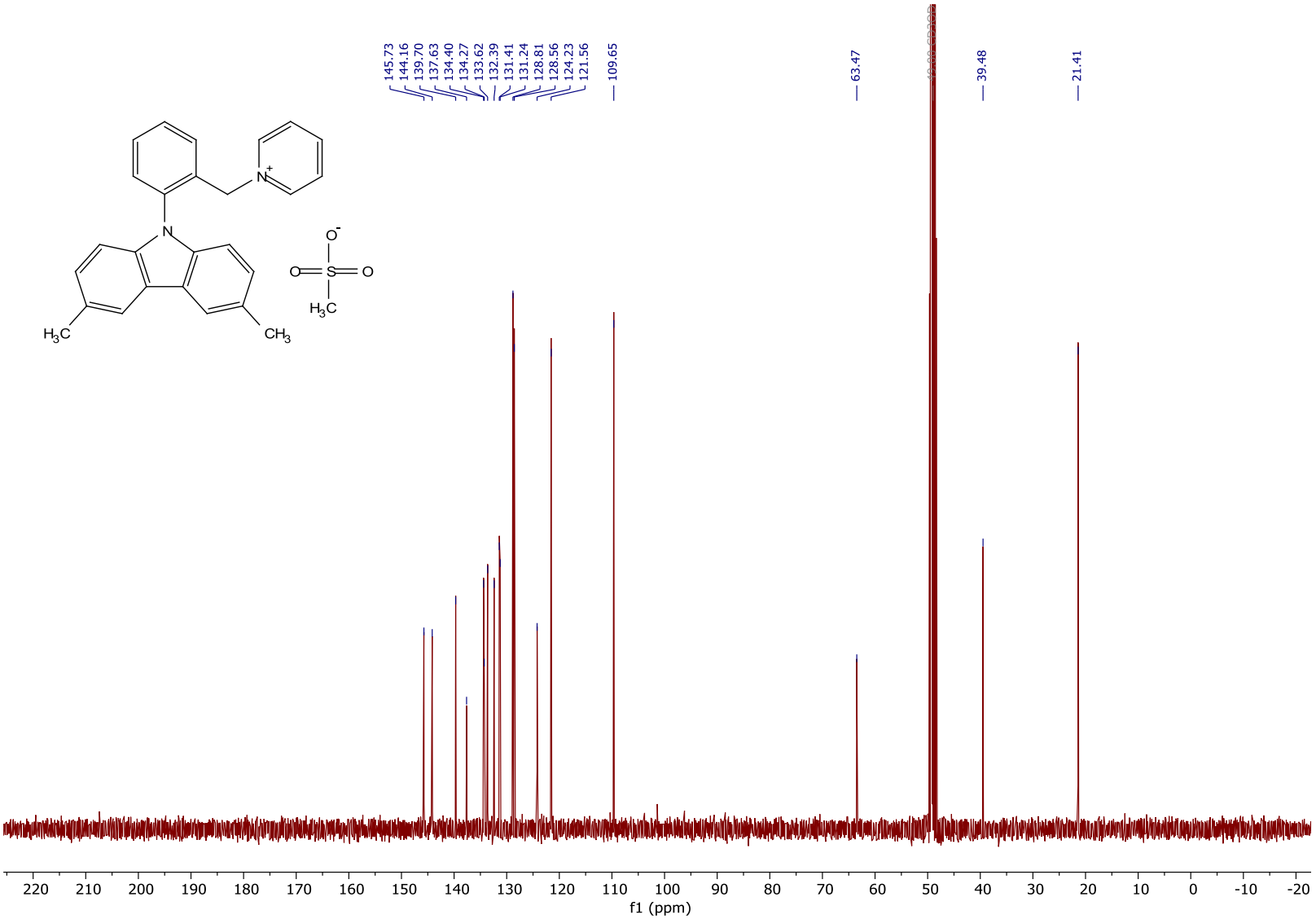

^{1}H NMR (400 MHz, CD_3OD, ppm) spectrum of 1-(2-(3,6-di-*tert*-butyl-9*H*-carbazol-9-yl)benzyl)pyridin-1-ium chloride (**4a**)

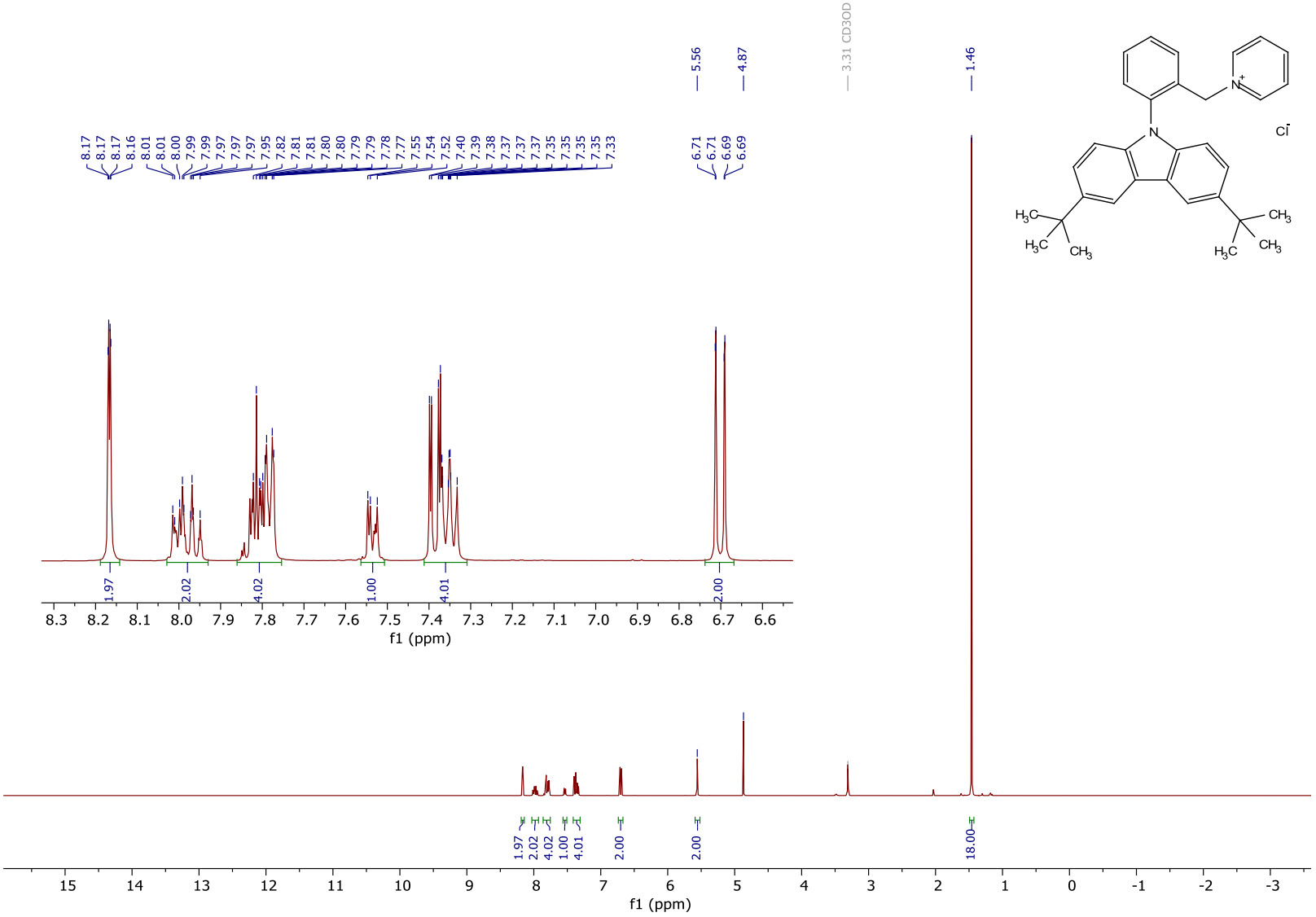

$^{13}C\{^{1}H\}$ NMR (101 MHz, CD_3OD, ppm) spectrum for 1-(2-(3,6-di-*tert*-butyl-9*H*-carbazol-9-yl)benzyl)pyridin-1-ium chloride (**4a**)

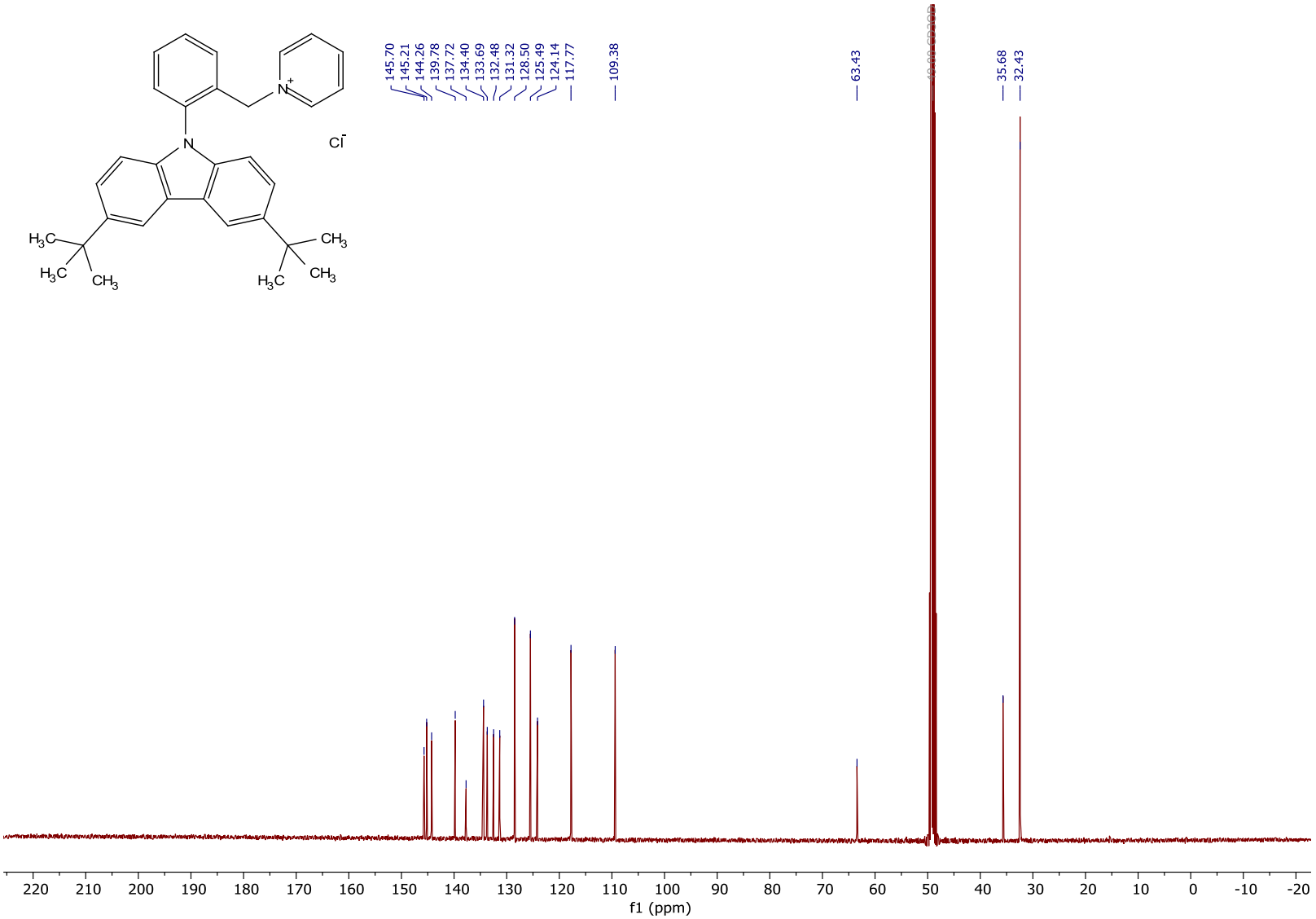

^{1}H NMR (400 MHz, CD_3OD, ppm) spectrum of 1-(2-(3,6-di-*tert*-butyl-9*H*-carbazol-9-yl)benzyl)pyridin-1-ium perchlorate (**4b**)

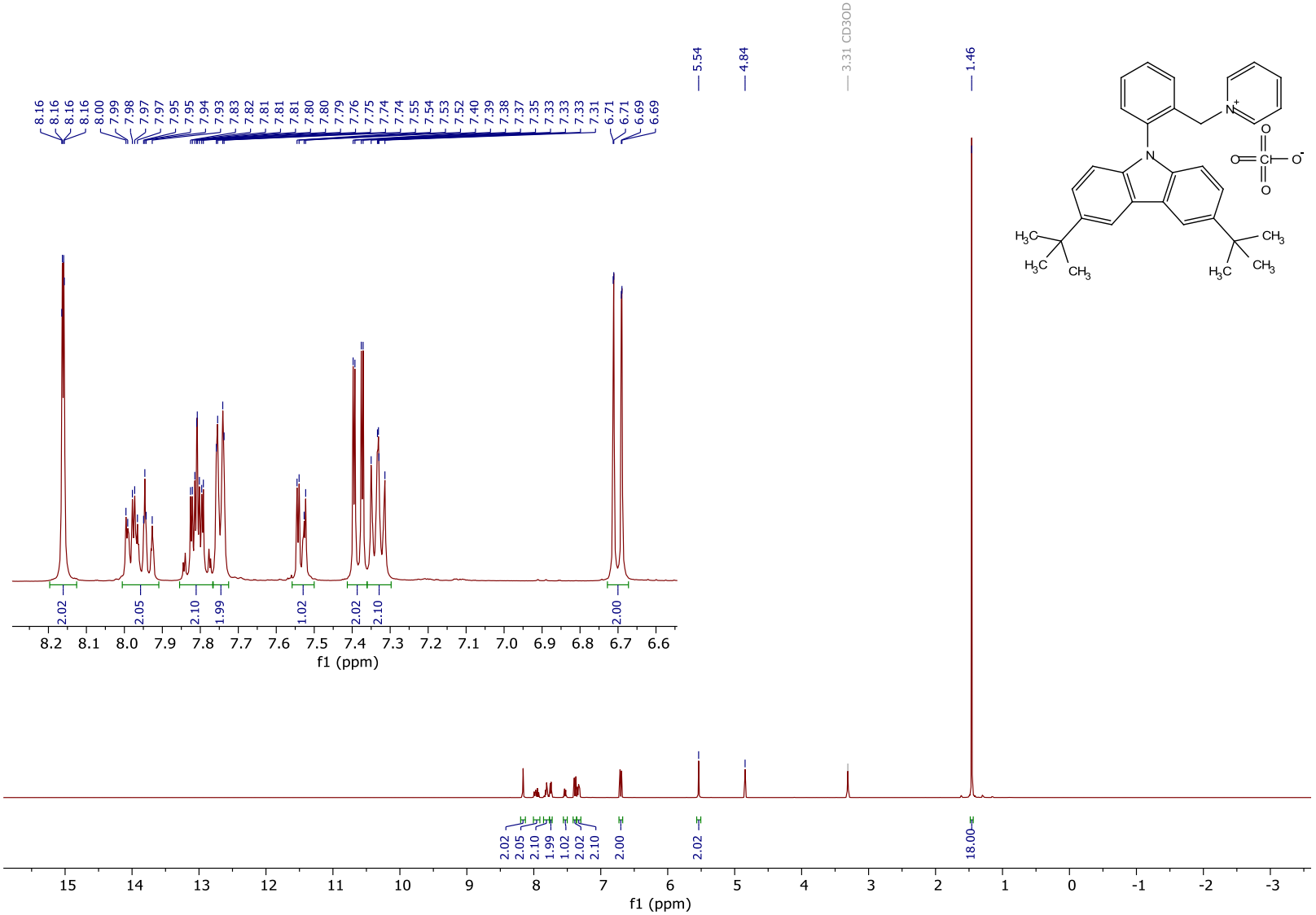

$^{13}C\{^{1}H\}$ NMR (101 MHz, CD_3OD, ppm) spectrum of 1-(2-(3,6-di-*tert*-butyl-9*H*-carbazol-9-yl)benzyl)pyridin-1-ium perchlorate (**4b**)

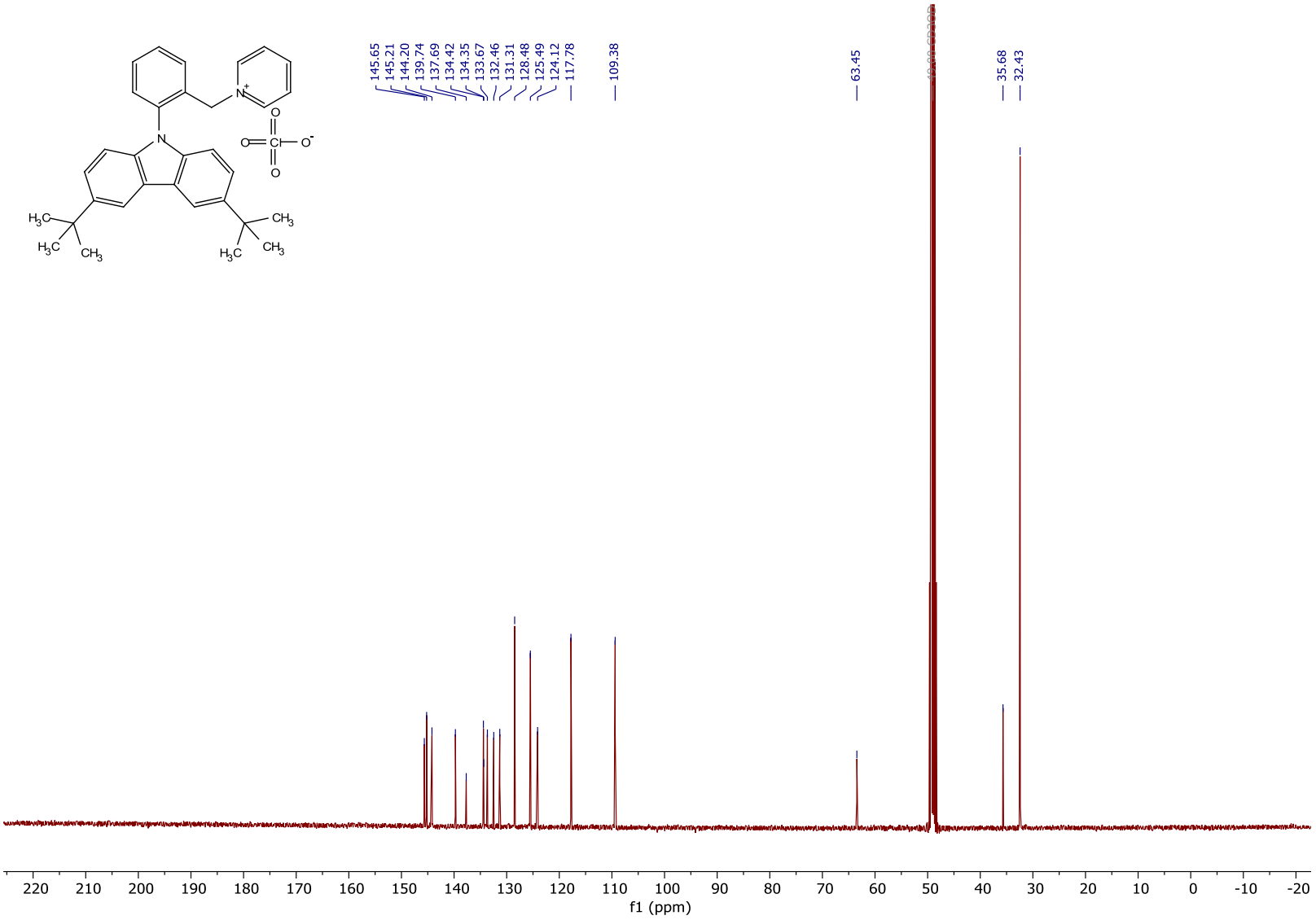

^{1}H NMR (400 MHz, $CDCl_3$, ppm) spectrum of ethyl 2-(9*H*-carbazol-9-yl)benzoate (**9**)

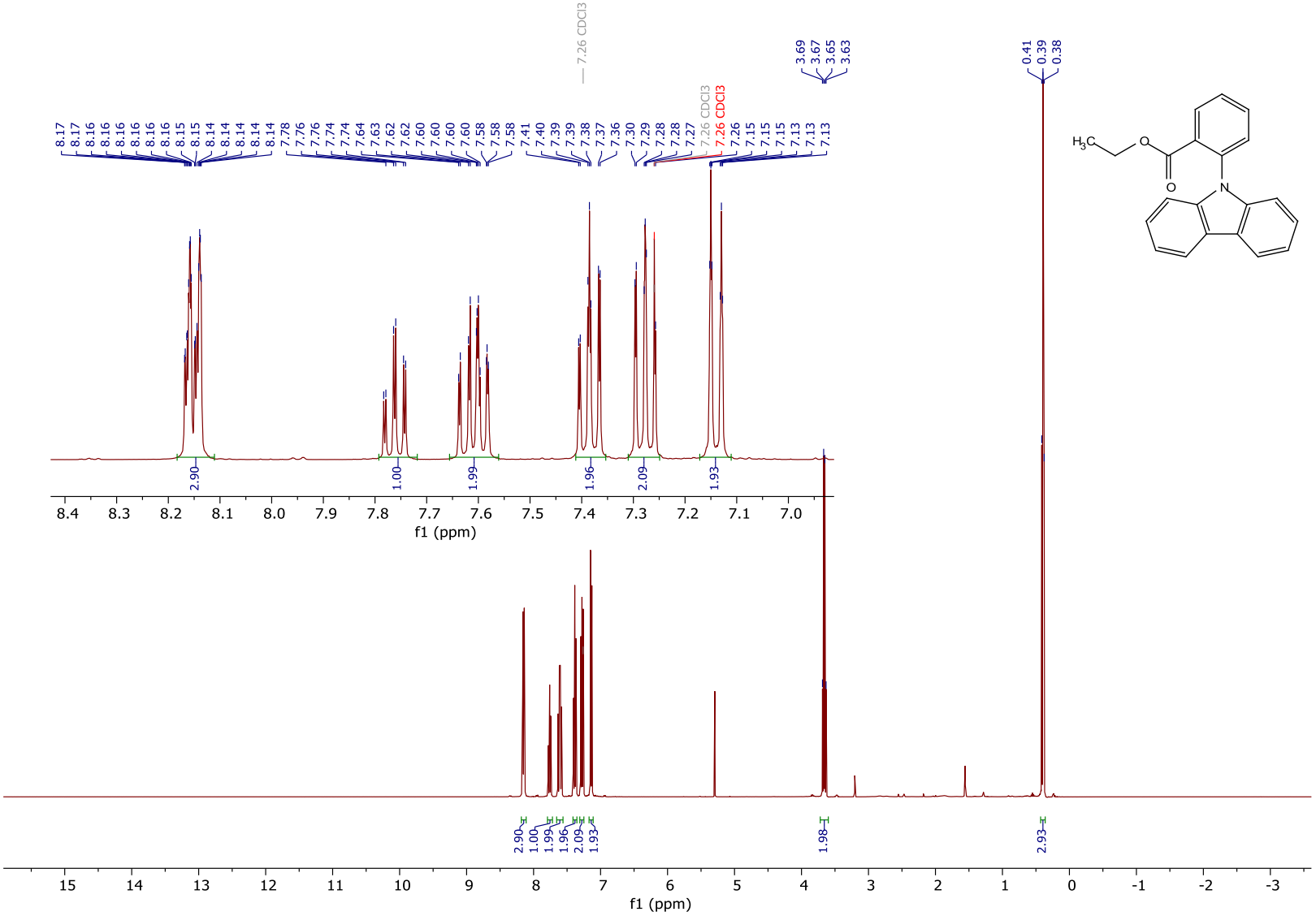

$^{13}C\{^{1}H\}$ NMR (101 MHz, $CDCl_3$, ppm) spectrum of ethyl 2-(9*H*-carbazol-9-yl)benzoate (**9**)

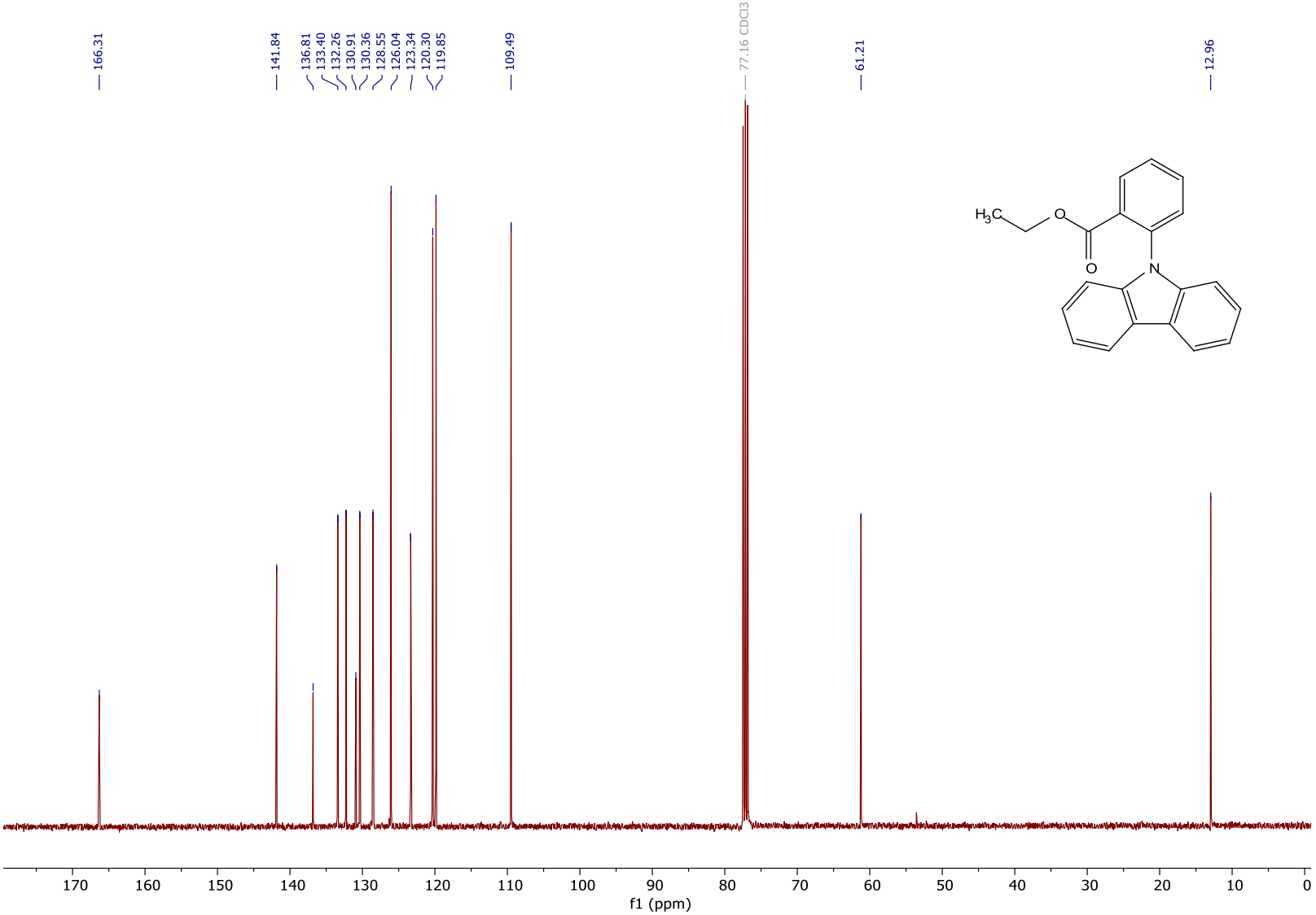

^{1}H NMR (400 MHz, $CDCl_3$, ppm) spectrum of ethyl 2-(3,6-dimethyl-9*H*-carbazol-9-yl)benzoate (**10**)

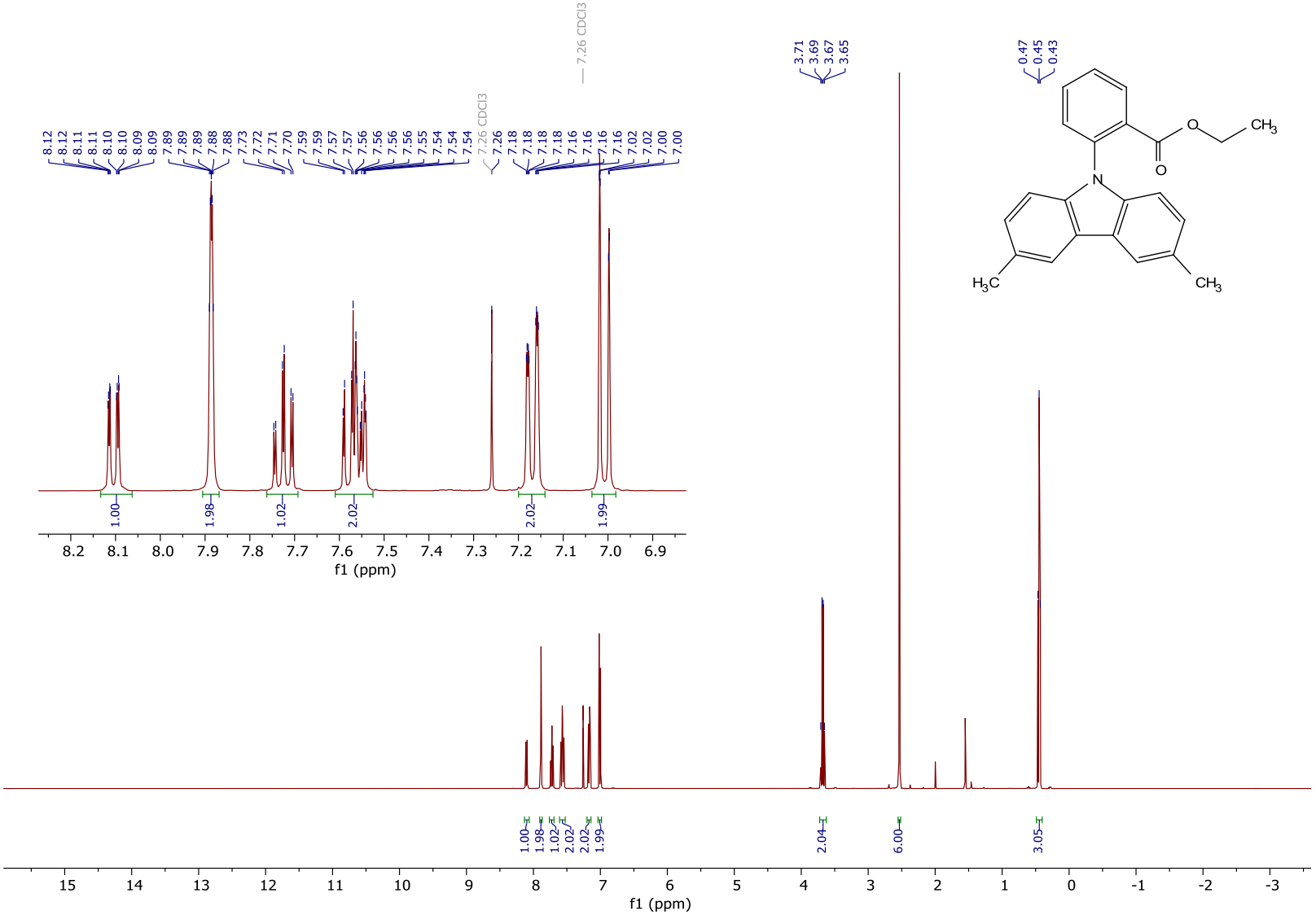

$^{13}C\{^{1}H\}$ NMR (101 MHz, $CDCl_3$, ppm) spectrum of ethyl 2-(3,6-dimethyl-9*H*-carbazol-9-yl)benzoate (**10**)

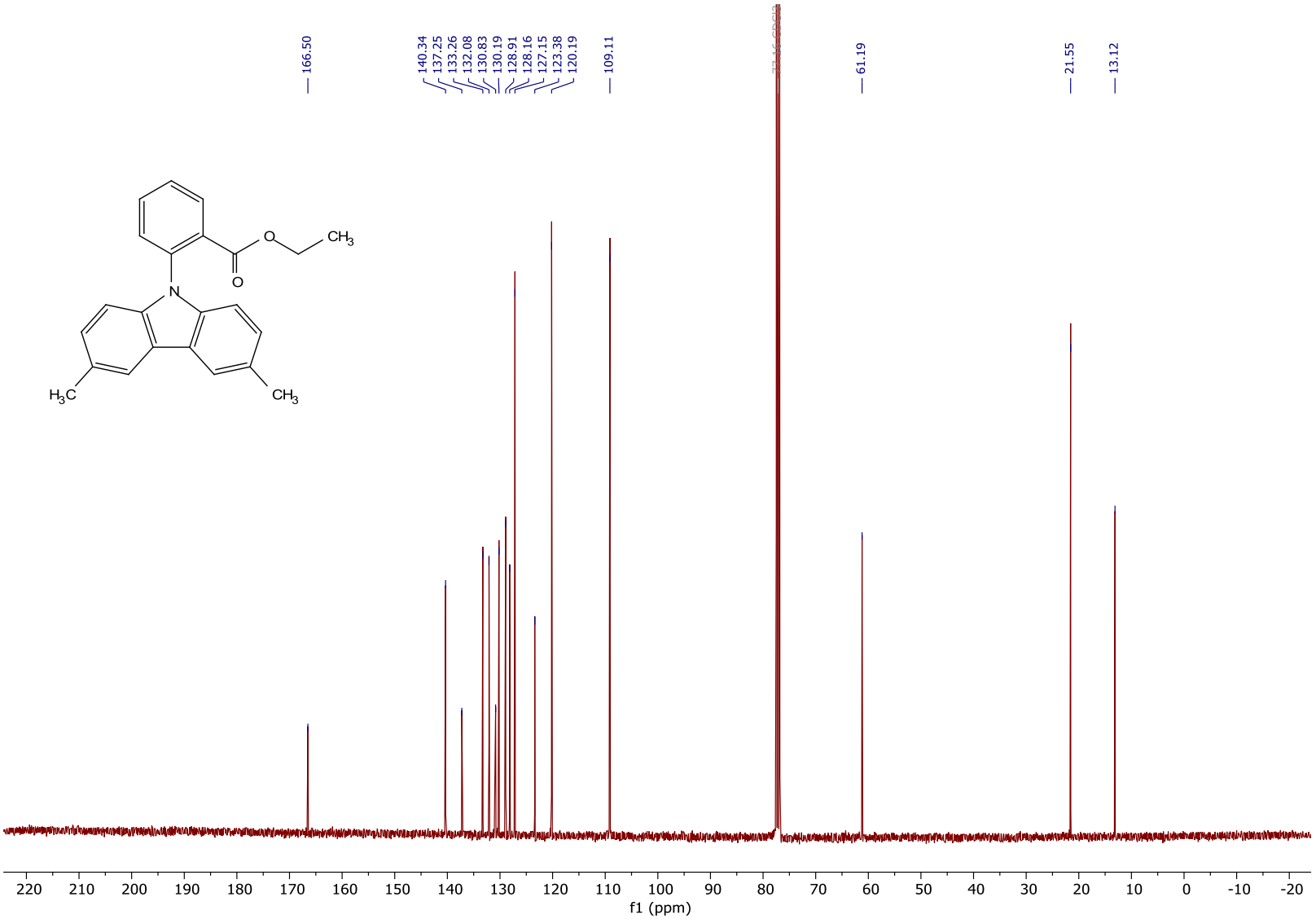

^{1}H NMR (400 MHz, $CDCl_3$, ppm) spectrum of ethyl 2-(3,6-di-*tert*-butyl-9*H*-carbazol-9-yl)benzoate (**11**)

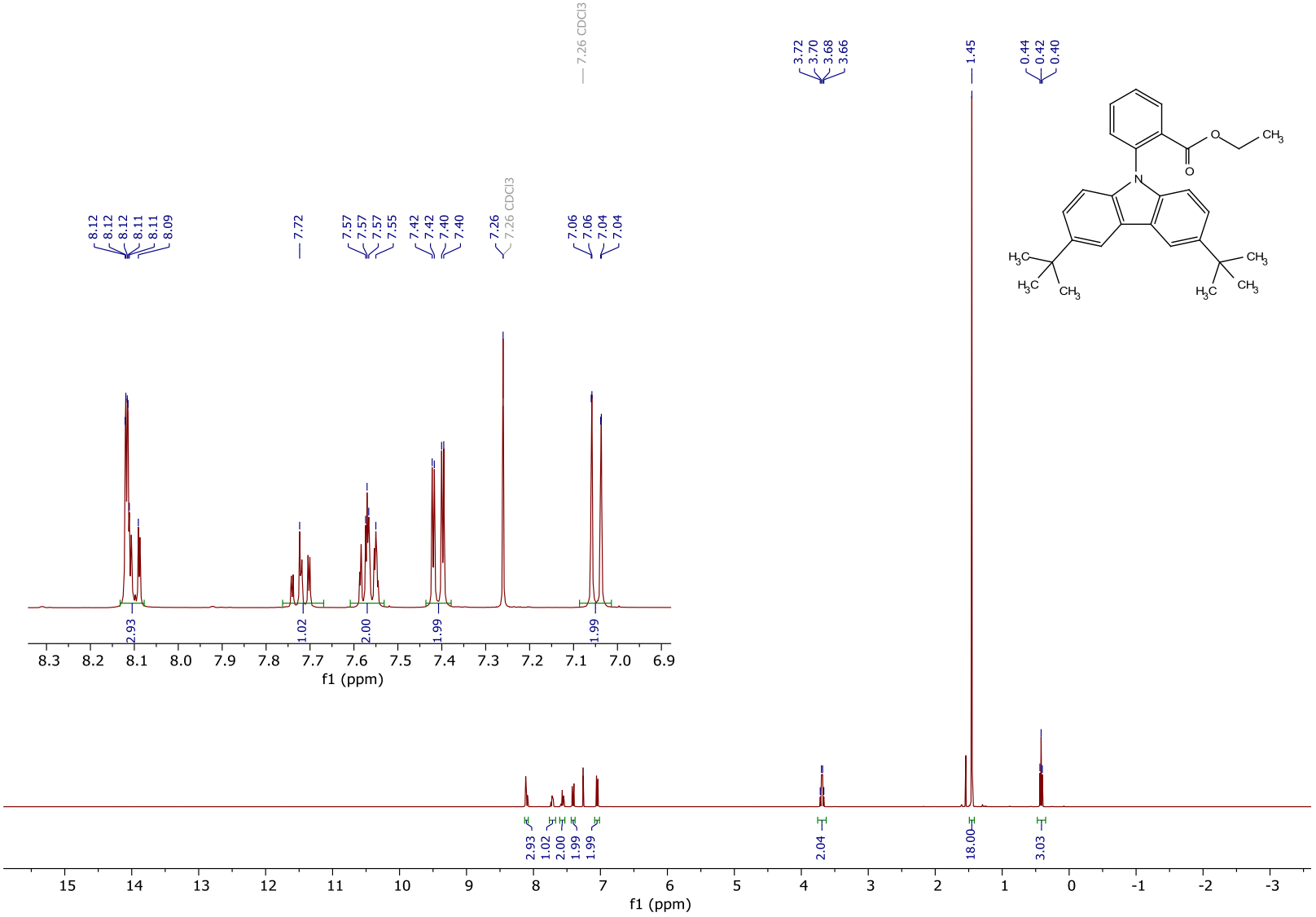

$^{13}C\{^{1}H\}$ NMR (101 MHz, $CDCl_3$, ppm) spectrum of ethyl 2-(3,6-di-*tert*-butyl-9*H*-carbazol-9-yl)benzoate (**11**)

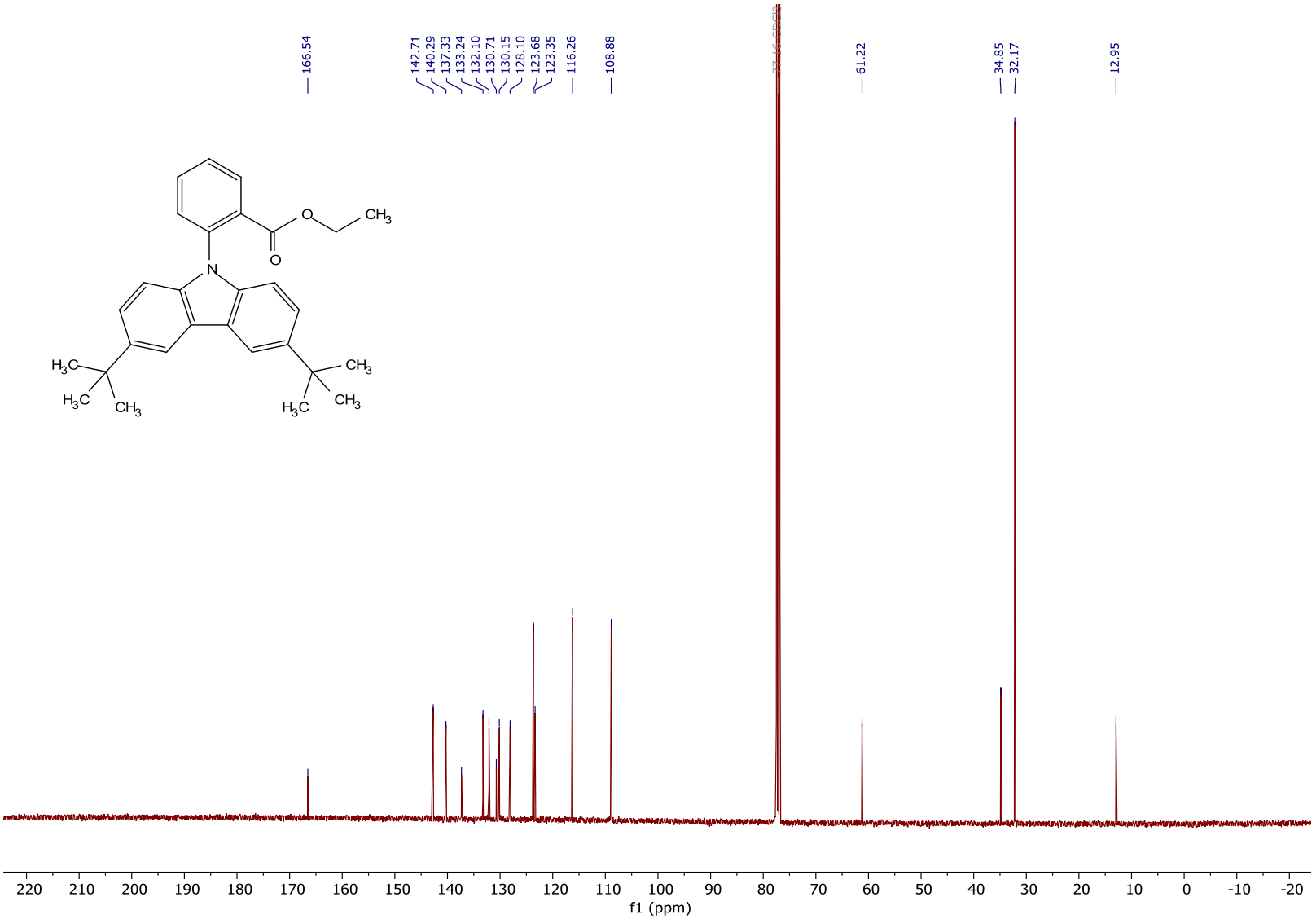

^{1}H NMR (400 MHz, $CDCl_3$, ppm) spectrum of (2-(9*H*-carbazol-9-yl)phenyl)methanol (**12**)

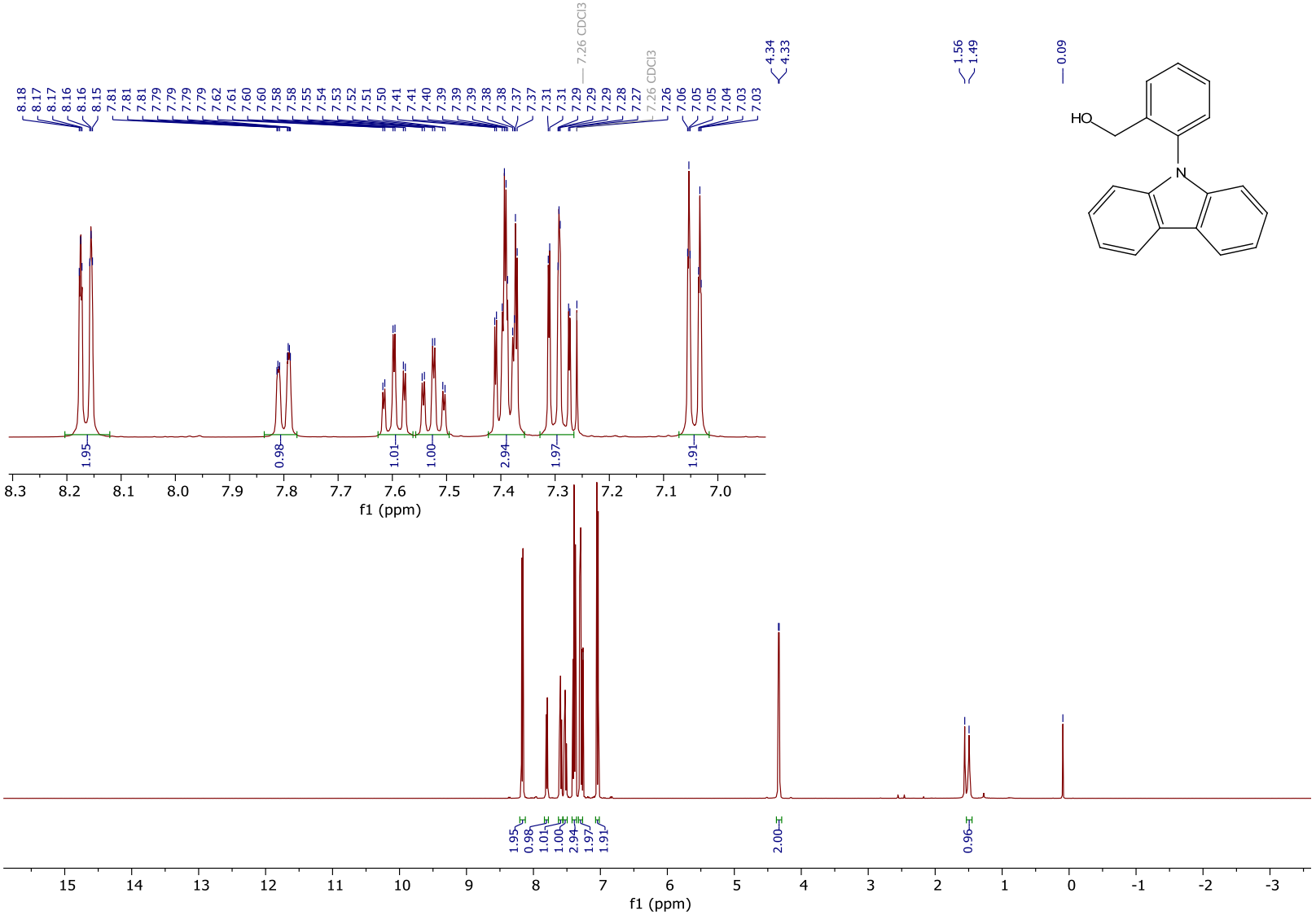

$^{13}C\{^{1}H\}$ NMR (101 MHz, $CDCl_3$, ppm) spectrum of (2-(9*H*-carbazol-9-yl)phenyl)methanol (**12**)

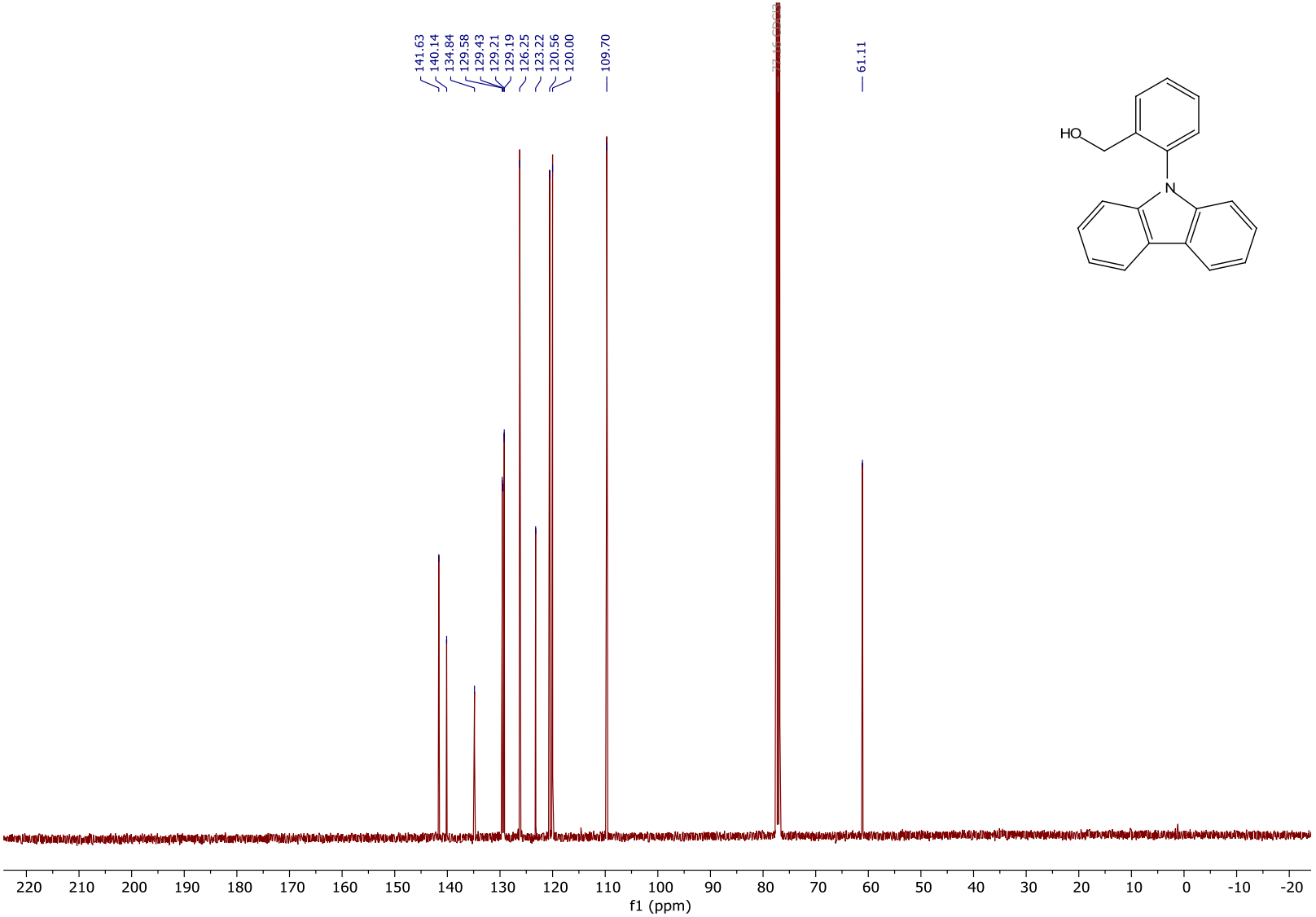

^{1}H NMR (400 MHz, $CDCl_3$, ppm) spectrum of (2-(3,6-dimethyl-9*H*-carbazol-9-yl)phenyl)methanol (**13**)

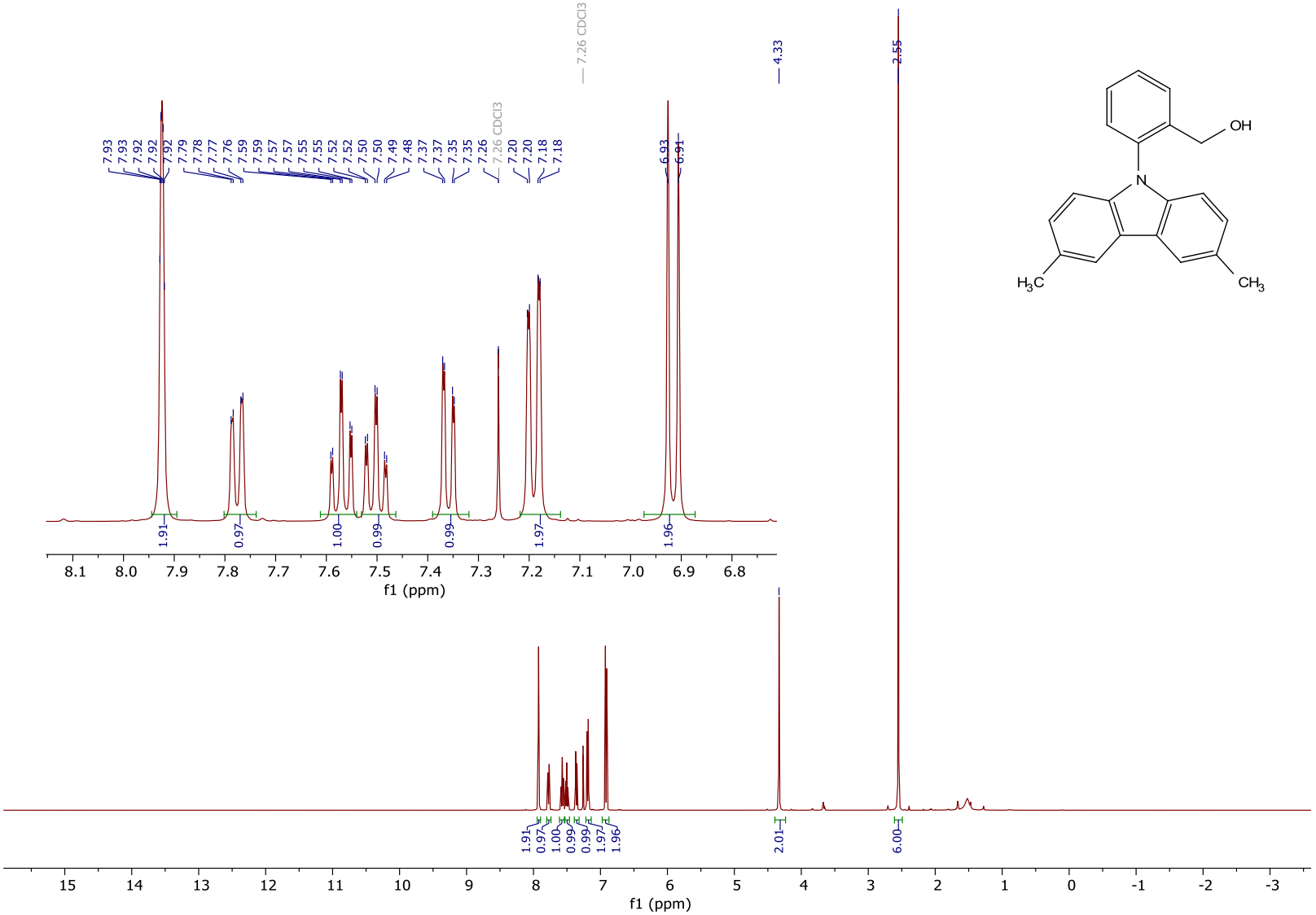

$^{13}C\{^{1}H\}$ NMR (101 MHz, $CDCl_3$, ppm) spectrum of (2-(3,6-dimethyl-9*H*-carbazol-9-yl)phenyl)methanol (**13**)

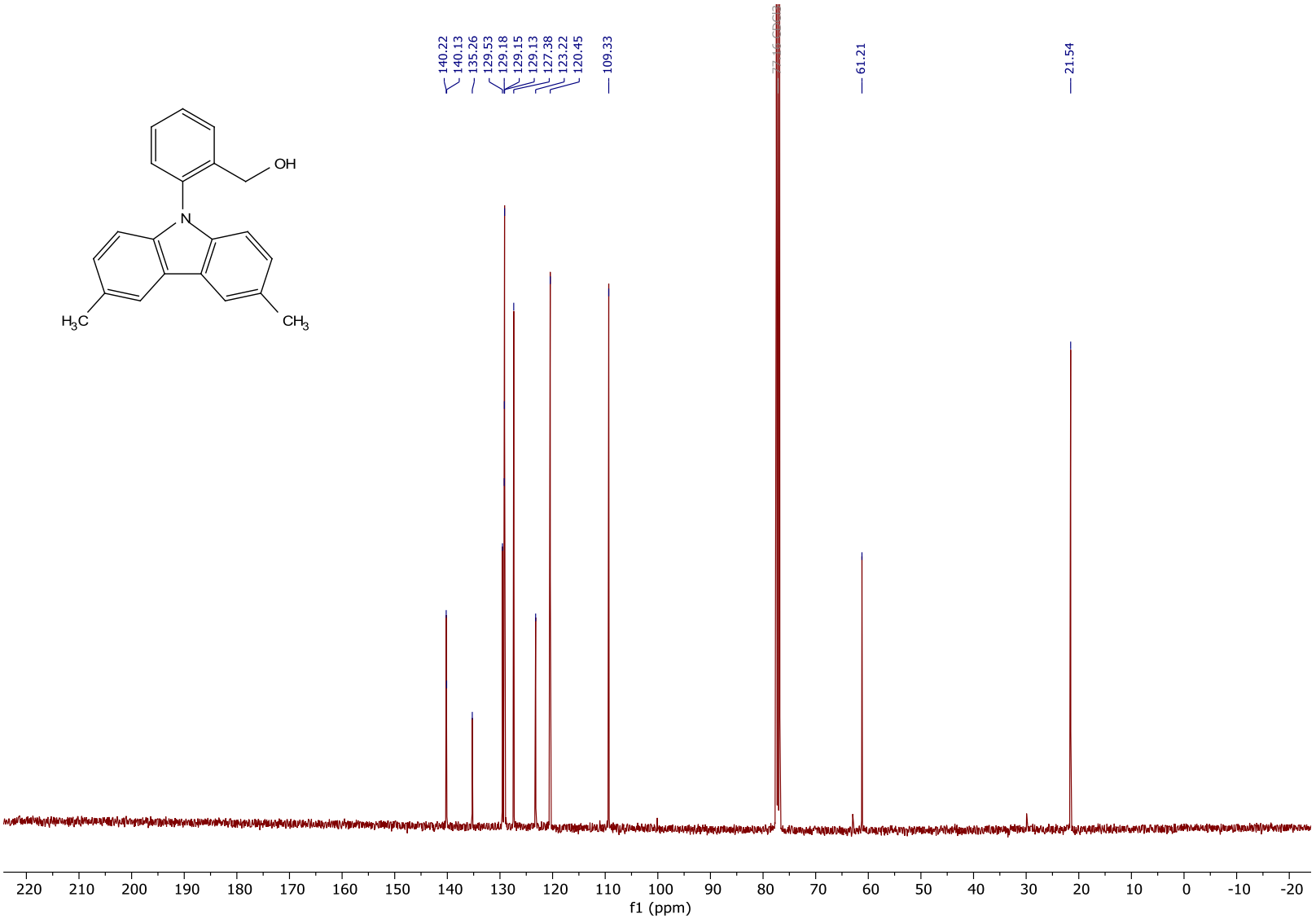

^{1}H NMR (400 MHz, $CDCl_3$, ppm) spectrum of (2-(3,6-di-*tert*-butyl-9*H*-carbazol-9-yl)phenyl)methanol (**14**)

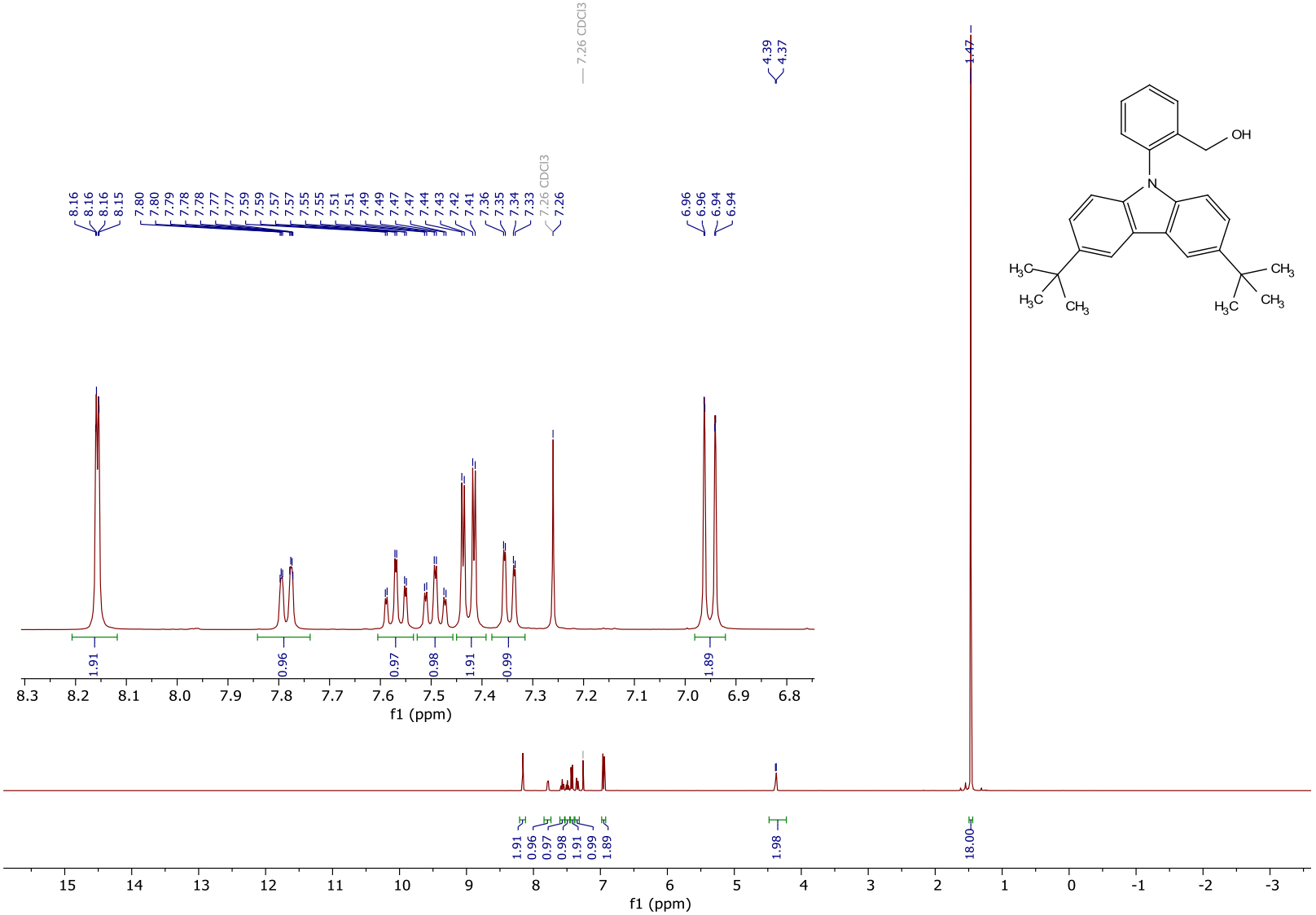

$^{13}C\{^{1}H\}$ NMR (101 MHz, $CDCl_3$, ppm) spectrum of (2-(3,6-di-*tert*-butyl-9*H*-carbazol-9-yl)phenyl)methanol (**14**)